Suarez, D.L. 2012. Modeling transient root zone salinity (SWS Model). In: W.W. Wallender and K.K. Tanji (eds.) Agricultural Salinity Assessment and Management. ASCE Manual and Reports on Engineering Practice No. 71 (2nd Edition). ASCE, Reston, VA. Chapter 28 pp:855-897.

CHAPTER 28

MODELING TRANSIENT ROOTZONE SALINITY (*SWS* MODEL)

Donald L. Suarez

INTRODUCTION

Modeling processes in soils serves multiple purposes. Most models are developed for either regulatory or management purposes, in which case they should be easy to use and have readily available input requirements. The management models usually contain a set of simplified and generalized scientific relationships but may sometimes be exclusively statistical and thus without explicit description of processes. Alternatively, models developed for research purposes consider a set of known or hypothesized processes serving as a tool for data analysis and thus furthering the scientific understanding of processes. Some take the position that all models, but especially management models, should be as simple as needed to represent the data. The difficulty with this approach is that unless the data set is extremely robust, only a limited set of conditions are examined and thus represented in the model. In this instance, locations with different specific conditions may result in unsatisfactory predictions. Most modeling efforts result in simulation of existing data, with the modeler adjusting input parameters, enabling a satisfactory match between the model and the data. Such an approach is of very little use as a management tool, where predictive capability is required and the collected data may not be sufficient to allow for validation.

Adding more complexity to a model, even if the science is correctly represented in the mathematical relationships, it may not necessarily improve the absolute predictive capability of the model. However, the advantage of a model based on tested algorithms of processes is that a user can evaluate the impact of changes on those processes. If the model has incorporated the major processes controlling the system, then the

model will be able to provide predictions of the system response to changes and thus serve as a valuable management tool. The objective of a management model should thus be to represent the underlying process, without undue burden on the user for collection of site-specific characterization or parameter information.

In this chapter we describe the development of rootzone salinity models, the *SWS* (Soil-Water-Salinity) salinity model and processes used by the model, as well as applications to management of saline soils or waters.

MODEL DEVELOPMENT

Both steady-state and transient models have a place in management of saline soils and waters. Steady-state models are easier to use and provide information about the long-term effect of a given change, such as the effect of a different irrigation water on soil properties. These models will input data, such as the average irrigation water volumes and concentrations, and average evapotranspiration (ET), and will calculate average yearly leaching fraction (LF) and soil salinity.

Transient models provide detailed information on temporal changes; this can be either unneeded detail (if the time scale of the change is exceedingly short) or critical (if the change is at a time frame that impacts other parts of the system, such as plant response to salt stress). As will be demonstrated, transient modeling is not just consideration of the transition from one steady state to another but, rather, analysis of the continual dynamic change experienced by natural systems. Depending on the scale of the changes, steady state can be considered for systems with seasonal fluctuations, but some processes, for instance, plant response to water salinity or toxic ions, may occur on a much shorter time scale.

The initial salinity models considered either mass balances of either water or chemicals. These models are still used, primarily for analysis of large scale systems, such as irrigation districts or hydrologic basins. Among these models are the *ASTRAN* model, (Labadie and Khan 1979) and the *Hydrosalinity* model, which also considers gypsum dissolution-precipitation (Quilez et al. 2011; Chapter 30 of this manual). Both of these models have been applied for salinity management at the basin scale.

Subsequently, rootzone water and chemical steady-state models were developed and then transient flow models. Hanks and Bowers (1962) developed a numerical solution for description of variably saturated water flow. Chemical models also evolved from mass balance models to thermodynamic equilibrium models, to models with kinetic considerations. Dutt (1962) developed a computer program to predict gypsum sol-

ubility coupled with cation exchange. Truesdell and Jones (1974) developed the *WATEQ* mineral equilibrium model, enabling determination of the mineral saturation status of waters.

Bresler (1973) described modeling of water and nonreactive solutes (coupled water and solute flow) under transient unsaturated flow conditions. Robbins et al. (1980) developed a combined chemical model considering cation exchange and calcite and gypsum equilibria coupled with variable water flow. This approach was further developed by Wagenet and Hutson (1987), into *LEACHM*, a model that is still widely utilized.

Suarez and Šimůnek (1992, 1997) described the *UNSATCHEM* model, which has similar objectives to *LEACHM* (with combined water flow, cation exchange, and equilibrium expressions for calcite and gypsum) but with added processes and interactions. Among the unique features, the model includes descriptions of kinetic expressions for calcite, a CO_2 production and transport routine for prediction of CO_2 concentrations needed for pH prediction, a boron (B) transport routine that considers adsorption-desorption as a function of pH, application of Pitzer expressions (Pitzer 1973; Felmy 1990) for ion activity calculations at high ionic strength and calculation of osmotic pressure, as well as a routine describing the impact of chemical properties [electrical conductivity (EC), sodium adsorption ratio (SAR), and pH] on the soil hydraulic properties.

The outputs from the various models are not always in agreement (Suarez and Dudley 1998) due to assumptions made regarding system response. For example, work by Robbins et al. (1980) and the initial *LEACHM* model (Wagenet and Hutson 1987) assume a fixed input CO_2 but do not properly predict soil pH and alkalinity changes, apparently due to the numerics of the calcite routine, which is only clearly evident with irrigation of high-alkalinity waters (Suarez and Dudley 1998). Current versions of *LEACHM* have corrected this problem (J. L. Hutson, personal communication, April 2008). The Dutt et al. (1972) model assumed that the soil is a closed system (no transfer of material in or out of the system) with respect to CO_2. The model predicts that the pH increases and the CO_2 concentration decreases as the water content increases and calcite is dissolved. This is correct for a closed system (such as soil and water in a closed flask over a short time interval), but the prediction is contrary to field observations (Buyanovsky and Wagner 1983) and considerations that there is gas exchange between the soil and the atmosphere.

Most models consider a fixed soil pH or fixed CO_2 (specified by the user). The fixed pH assumption is reasonable only for extremely short-term simulations or where the water composition remains constant. The fixed-CO_2 assumption is preferable to the closed-system assumption and to the fixed-pH assumption because it allows prediction of the impact of water composition and mineral reactions on soil pH. It is reasonable to

assume that the chemical reactions have a minimal impact on the gas composition in soil; thus, the gas composition can be defined outside of the chemical system. However, as discussed in the following sections, the fixed-CO_2 assumption may be adequate for a steady-state model, but the CO_2 concentration is not constant because the soil is a dynamic system, where the gas concentration is defined by the processes of production and transport. The *UNSATCHEM* model predicts that as the water content increases, the CO_2 transport out of the rootzone is decreased and the CO_2 concentration increases. These predictions are consistent with observations of O_2 depletion under wet conditions. Following are descriptions of some of the relevant processes.

SWS MODEL

The *SWS* model was developed as a user-friendly transient-water-flow chemistry model for salinity management. The modeling approach is deterministic in that it is based on a set of mathematically defined process such that with each set of data input a unique and reproducible prediction is obtained (Addiscott and Wagenet 1985). The base of the program is that of *UNSATCHEM* (Suarez and Šimůnek 1992, 1997) with addition of calculations for ET, a new B adsorption routine, and with a user-friendly interface that makes extensive use of default parameters to minimize the need for user expertise in soil physics and chemistry.

Water Flow

Hydraulic functions

The *SWS* model uses a modified version of the one-dimensional Richards' equation:

$$\frac{\partial \theta_w}{\partial t} = \frac{\partial}{\partial z}\left[k\left(\frac{\partial h}{\partial z} - 1\right)\right] - S \qquad (28\text{-}1)$$

where h is the water pressure head, θ_w is the volumetric water content, k is the hydraulic conductivity, t is time, z is the depth coordinate, and S is the sink term, representing extraction of water from the soil by plant roots. The effects of thermal and density gradients on water flow are neglected, and it is further assumed that the gas phase dynamics do not affect water flow. These simplifications are not justified in all instances. For example, density gradients can be significant when saline waters are present, but consideration of these processes increases the complexity beyond the scope of this already complex model.

The unsaturated soil hydraulic properties are described by a modified version of those proposed by van Genuchten (1980). The water retention and hydraulic conductivity (HC) functions are given by

$$\theta(h) = \theta_r + \frac{\theta_s - \theta_r}{(1 + |\alpha h^n)^m} \tag{28-2}$$

and

$$K(h) = K_s K_r r = K_s r S_e^{1/2}[1 - (1 - S_e^{1/m})^m]^2 \tag{28-3}$$

respectively, where

$$m = 1 - 1/n \qquad n > 1 \tag{28-4}$$

and

$$S_e = \frac{\theta - \theta_r}{\theta_s - \theta_r} \tag{28-5}$$

where θ_r and θ_s are the residual and saturated water content (expressed as $cm^3 cm^{-3}$), respectively, K_s is the saturated conductivity [cm d^{-1}], K_r is the relative HC (scaled from 0 to 1), S_e is relative saturation, and m, n, and α [cm^{-1}] are the empirical parameters of the hydraulic characteristics. In order to increase numerical stability in the range of h from 0 to −2 cm, we specify a constant $\theta(\theta_s)$ for that interval. Hydraulic characteristics are determined by the set of six parameters, θ_r, θ_s, α, n, K_s, and the unique variable r, representing a reduction function (scaled from 0 to 1) describing the effect of soil chemistry on hydraulic properties and is discussed in more detail later. Use of the model requires optimizing the first five parameters from the experimental water retention, pressure head, and saturated conductivity data.

It is not realistic to expect users of a management model to conduct detailed studies on the water retention curve and unsaturated HC of each soil considered. For use in a crop-irrigation management model, the water retention versus pressure head curve can be approximated by the functions obtained from soil texture (Carsel and Parrish 1988), and thus are included in the interface of the present model. The estimates of saturated HC given in this data set are likely the major error for our applications to irrigated agriculture. The saturated HC is important because water or rain applied at a rate in excess of infiltration may result in surface runoff and thus infiltration below the applied amount. In some instances the values presented by Carsel and Parrish (1988) appear greater than what we

observe locally, for example, K_s for a loam soil. In this instance, it is suggested that the user maintain the water retention versus pressure head curve of the default parameters based on the soil texture (Carsel and Parrish 1988) and then input their own or local estimates of K_s for their soil. Alternatively, users with hydraulic information can use the advanced option and input their own hydraulic parameters.

Chemical effects on hydraulic conductivity

It is well known that soil hydraulic properties are affected by chemical properties of the soil, but to date this is not accounted for in other models. Equation 28-3 differs uniquely from previous hydraulic expressions in that it includes a reduction term, r, which scales the HC in relation to the EC, pH, and SAR conditions in the soil. Optimal soil chemical conditions for infiltration are represented by values of $r = 1$. Elevated levels of exchangeable Na result in swelling of smectitic clays, detachment of clay particles, dispersion, and subsequent clay migration and redeposition. All of these processes result in blocking of pores at low salinity and in the presence of exchangeable sodium (McNeal 1968; Shainberg and Levy 1992). These processes are observed in the natural development of clay pan layers in soils and, more dramatically, in sodic, nonsaline soils. In addition, elevated levels of pH adversely affect saturated HC, separate from the sodicity and salinity interactions (Suarez et al. 1984).

Suarez and Šimůnek (1997) represented the chemical effects on hydraulic properties by the use of a reduction function, r, given by

$$r = r_1 r_2 \tag{28-6}$$

where r_1 is the reduction due to the combined adverse effects of low salinity and high exchangeable sodium fractions on the clay, and r_2 is the adverse effect of pH. The r_1 term is given by McNeal (1968) as

$$r_1 = 1 - \frac{cx^n}{1 + cx^n} \tag{28-7}$$

where c and n are empirical factors, and x is defined by

$$x = f_m\, 3.6 \times 10^{-4}\, ESP^*\, d^* \tag{28-8}$$

where f_m is the mass fraction of smectite (defined as montmorillonite and beidellite) in the soil, d^* is an adjusted interlayer mineral spacing, and ESP^* is an adjusted exchangeable sodium percentage (percentage of

the total cation exchange charge neutralized by Na^+). The term d^* is defined by

$$\begin{aligned} d^* &= 0 && C_0 > 300 \text{ mmol}_c\text{L}^1 \\ d^* &= 356.4(C_0)^{-0.5} + 1.2 && C_0 \leq 300 \text{ mmol}_c \text{ L}^1 \end{aligned} \tag{28-9}$$

where C_0 is the total salt concentration of the solution, and the term ESP^* is given by

$$ESP^* = ESP_{soil} - (1.24 + 11.63 \log C_0) \tag{28-10}$$

The reduction factor r_2, representing the effect of pH on HC, was calculated from the SAR-pH saturated HC experimental data given in Suarez et al. (1984). The data were first corrected for the effects of salinity and exchangeable sodium using the r_1 values calculated from the aforementioned. Based on this limited data,

$$\begin{aligned} r_2 &= 1 && \text{for pH} < 6.83 \\ r_2 &= 3.46 - 0.36 \text{ pH} && \text{for } 6.86 \leq \text{pH} \leq 9.3 \\ r_2 &= 0.1 && \text{for ph} > 9.3 \end{aligned} \tag{28-11}$$

In view of the differences among soils, these specific values may not be generalized predictors of soil HC, but they do represent conditions of arid land soils examined at the U.S. Salinity Laboratory. The response of soil hydraulic properties to pH has not been extensively studied, but it is reasonable to assume that soils differ in their reaction to these factors. This option in the model should *not* be considered as a quantitative prediction of what will occur at a specific site but is useful to evaluate the relative importance of the chemical effects under different soil and water conditions. Many other factors in addition to sodicity and pH affect soil aggregate stability, such as organic matter, soil texture, clay mineralogy, or tillage, and it is reasonable to assume that there are interactions between these factors and the chemical factors considered here.

By use of the reduction function it is implied that the relative response to sodic conditions, obtained under saturated conditions, is applicable to unsaturated conditions. This is likely not entirely correct, but for irrigated agriculture the most important water flow occurs at and near saturation (as water is applied) and the available data are entirely based on saturated flow experiments. Another important simplifying assumption is that the processes are reversible. This assumption is likely valid when the reduction in HC is due to swelling, but it is likely not valid when clay

dispersion occurs. The extent to which sodic reclamation restores HC (with or without tillage) is unknown. Extensive research on reclamation has focused primarily on chemical changes and secondarily on improvements in hydraulic properties relative to the initial degraded condition.

Plant Modeling

Water uptake by plant roots

Water uptake by plants is related to the rooting distribution. There are two options in the *SWS* model related to root distribution: a user-specified fixed root distribution and an initial user-specified distribution coupled to root growth. The fixed rooting distribution option is used when simulating perennial crops such as alfalfa and pasture grasses, but it can also be used for simplified input for annual crops.

Water uptake by plants is related to the rooting distribution, input ET, and water and salt stress simulated by the model. The model predicts relative yield based on the ratio of predicted ET_a, (actual ET calculated by the model after consideration of stress) to optimum ET_c, (optimum ET of the crop). The root growth option can be used for simulation of annual crops. In this case the user inputs an initial root distribution from which the roots will develop. This option requires additional inputs, such as initial rooting depth, maximum rooting depth, and growing degree days for the crop.

The sink term in Eq. 28-1 is the volume of water removed from a unit volume of soil per unit of time as a result of plant water uptake. The root water uptake in response to water and salinity stress is expressed as

$$S = S_p \alpha_s(h) \alpha_\varphi(h_\varphi) \tag{28-12}$$

where S_p is the potential water uptake [$cm^3 cm^{-3} d^{-1}$], $\alpha_s(h)$ is the water (matric) stress function, h is the matric head [m], $\alpha_\varphi(h_\varphi)$ is the osmotic stress function, and h_φ is the osmotic head [m]. As shown by Eq. 28-12, water uptake is obtained by multiplying the water stress reduction function, matric stress reduction function, and potential water uptake. The model calculates the stress functions and water uptake at each time step. There is uncertainty as to how to best represent the response to combined stresses, but the multiplicative approach appears preferable to the alternative addition of the osmotic and matric pressure and representation of a single stress function or the assumption that only the most limiting stress need be considered (see Grieve et al., Chapter 13 of this manual, for more discussion).

The water stress response function, $\alpha_s(h)$, is a dimensionless function of the soil water pressure head ($0 \leq \alpha_s(h) \leq 1$) described by van Genuchten (1987) as

$$\alpha_s(h) = \frac{1}{1 + \left(\frac{h}{h_{50}} \right)^p} \tag{28-13}$$

where h_{50} [m] and p are empirical constants. The default parameter of the model is set at h_{50} equal to -50 m and $p = 3$. The parameter h_{50} represents the pressure head at which the water extraction rate is reduced by 50%. Specific crop values of h_{50} are not available but a default value can be estimated from the wilting point. This water stress response function, $\alpha_s(h)$, does not consider transpiration reduction near saturation. The decrease in water uptake that is sometimes observed at saturation is related to oxygen stress and is more properly treated based on prediction of the gas phase composition (for models such as *SWS* that include CO_2 production and transport).

An expression similar to Eq. 28-13, only with $\alpha_\varphi(h_\varphi)$ and $h_{\varphi 50}$ for osmotic stress, is used for salinity:

$$\alpha_\varphi(h_\varphi) = \frac{1}{1 + \left(\frac{h_\varphi}{h_{\varphi 50}} \right)^p} \tag{28-14}$$

Specific values of the $h_{\varphi 50}$ and p parameters for salinity are presented in the model for selected crops. If other crops are selected it is suggested that in the absence of detailed information, the $h_{\varphi 50}$ value be calculated from the more traditional Maas-Hoffman relationship (Grieve et al., Chapter 13 of this manual; Maas and Hoffman 1977). The Maas-Hoffman relationship represents data in terms of a threshold electrical conductivity (EC) or osmotic pressure above which there is a yield decline and a slope that describes the yield decline with increasing salinity (expressed in terms of EC or osmotic pressure). From the salt response threshold and slope, the $h_{\varphi 50}$ can be easily calculated and p can be set to 3.0.

The potential water uptake rate in the rootzone is expressed as the product of the potential transpiration rate, T_c [cm d^{-1}], and the normalized water uptake distribution function, $\beta(z)$ [cm^{-1}], where z is depth (cm). The normalized water uptake distribution function describes the variation with depth of the potential water uptake rate, S_p, over the rootzone, as follows:

$$S_p = \beta(z) T_c \tag{28-15}$$

For a fixed root distribution, the function $\beta(z)$ is specified by the user. The actual (calculated) transpiration T_a is given by

$$T_a = \int_{L-L_r}^{L} S(h, h_\varphi, z)dz = T_c \int_{L-L_r}^{L} \alpha_s(h)\alpha_\varphi(h_\varphi)\beta(z)dz \qquad (28\text{-}16)$$

The terms L and L_r are, respectively, the depth at the soil surface (0) and the depth of the deepest root. The total actual transpiration for each time interval is calculated by summation of the actual transpiration amounts for each of the rootzone depth intervals. The transpiration in each of the depth intervals is based on the root distribution function, the potential crop transpiration, and the stress calculated in that depth interval. There is currently no compensation at other depths for reduced water uptake within any depth interval. The total transpiration for the simulation is the sum of the actual transpiration time intervals. The ratio of actual transpiration to optimal transpiration is used to calculate the relative yield. This calculation does not currently consider the change in water use efficiency under salt stress. Changes in water use efficiency (unit fresh weight/unit of water consumed) related to salt stress are currently available for only a few crops and cannot be generalized because some increase and some decrease with increasing salinity.

The fixed root option is always selected for a perennial crop. It is also possible to use the fixed root option for predicting the water uptake and relative crop yield for an annual crop. In this instance, the input ET_c values are ET_0 multiplied by the crop coefficient. Values for these coefficients are crop- and locality-specific, as well as varying with time during growth, thus are ideally provided by the model user. Use of this option requires more detailed information but may provide more accurate prediction of water requirements and use if the crop factors are known for the crop and locality to be simulated. The user manual presents coefficient data on selected crops and at different stages of growth.

Water uptake by plant roots: root growth option

A specification of the root growth option enables use of a simplified crop-root growth model. In this instance, the input is still ET_c and this value must be input or calculated by the model. Additional plant-specific information is required, including planting date, growing degree days (GDD) to maturity, and harvest date. The plant is divided into various stages of development and the initial rooting depth must be specified. If the shallow initial rootzone dries out, there will be water stress. It is suggested that the user ensure that the initial conditions are reasonable with regard to the initial root distribution and the total amount of water extracted.

Root growth. The root depth, L_r, can be either constant or variable during the simulation. For annual vegetation, the plant submodel is required to simulate the change in rooting depth with time. In *UNSATCHEM* (Suarez and Šimůnek 1996, 1997) the root depth is the product of the maximum rooting depth, L_m [cm], and the root growth coefficient, $f_r(t)$:

$$L_r(t) = L_m f_r(t) \tag{28-17}$$

To calculate the root growth coefficient, $f_r(t)$, Šimůnek and Suarez (1993) combined the Verhulst-Pearl logistic growth function with the GDD function. The logistic growth function is used to describe biological growth at constant temperature, and the GDD model is utilized for determining the time between planting and plant maturity. The model uses a modified version of the GDD relation developed by Logan and Boyland (1983), who assumed that this function is fully defined by the temperature, T [K], expressed by a sine function approximating the temperature variation during the day, and by the three temperature limits, T_1, T_2, and T_3 [K]. When the actual temperature is below the base value T_1, plants do not grow. Plant growth is at a maximum rate at temperature T_2, with growth constant up to a maximum temperature T_3, above which increased temperature has an adverse effect on growth.

Based on this information, Šimůnek and Suarez (1993) developed the following dimensionless growth function:

$$g(t) = \begin{cases} g(t) = 0 & t \le t_p ; t \ge t_h \\ \dfrac{1}{T_{Bas}}\left[\int \delta(T - T_1)dt - \int \delta(T - T_2)dt - \int \delta(T - T_3)dt\right] & t \varepsilon (t_p, t_m) \\ g(t) = 1 & t \varepsilon (t_m, t_h) \end{cases} \tag{28-18}$$

where T_{Bas} are the heat units [KT] necessary for the plant to mature and the roots to reach the maximum rooting depth; t_p, t_m, and t_h represent time of planting, time at which the maximum rooting depth is reached and time of harvesting, respectively; and parameter δ is the reduction in optimal growth due to the water and osmotic stress. The expression inside the brackets of Eq. 28-18 equals T_{Bas} at time t_m when roots reach the maximum rooting depth. The individual integrals in Eq. 28-18 are evaluated only when the arguments are positive. Parameter δ is defined as the ratio of the actual to potential transpiration rates:

$$\delta = \frac{T_a}{T_p} \tag{28-19}$$

Biomass and/or root growth is represented with the Verhulst-Pearl logistic growth function:

$$f_r(t) = \frac{L_0}{L_0 + (L_m - L_0)e^{-rt}} \tag{28-20}$$

where L_0 is the initial value of the rooting depth at the beginning of the growth period [cm] and r is the growth rate [cm d^{-1}].

Combining the concepts for GDD (Eq. 28-18) and logistic growth (Eq. 28-20), the time to maturity is expressed as (Šimůnek and Suarez 1993)

$$t = t_m g(t) \tag{28-21}$$

where t_m is the time when GDD reaches the specified plant species heat units for maturity (T_{Bas}).

Calculations of Crop Evapotranspiration

Water consumption at any time step is calculated based on ET_c and the stress reduction factor. In the absence of input ET_c information, the model will predict ET_c using the FAO version of the Penman-Monteith equation (Allen et al. 1998), given as

$$ET_0 = \frac{0.408\Delta(R_n - G) + \gamma\left(\frac{900}{t+273}\right)U_2(e_s - e_a)}{10(\Delta + \lambda(1 + 0.34U_2))} \tag{28-22}$$

where ET_0 is expressed in cm/day, Δ is the slope of the saturation vapor pressure curve (kPa $°C^{-1}$), R_n is the net radiation at the crop surface (MJ $m^{-2}d^{-1}$), G is the soil heat flux density (MJ $m^{-2}d^{-1}$), γ is the psychrometric constant (kPa $°C^{-1}$), t is the mean daily air temperature (°C), e_s is the saturation vapor pressure (kPa) at the specified temperature, e_a is the measured or calculated vapor pressure, and U_2 is the wind speed at a height of 2 m above the surface (m s^{-1}). The terms on the right side of Eq. 28-22 are all calculated using the expressions given in *FAO Irrigation and Drainage Paper 56* (Allen et al. 1998).

The input variables needed to calculate ET_0 using this approach can be reduced to wind speed, latitude, elevation, calendar date, mean daily temperature, daily temperature fluctuation, fraction of the day that is clear, and maximum relative humidity—all factors that should be readily available on a daily basis.

Crop coefficients and calculation of ET_c

Crop coefficients (k_c) serve to convert the ET_0 values into ET_c for the crops of interest. The reference ET_0 is for a hypothetical crop with an

assumed height of 0.12 m having a surface resistance of 70 s m^{-1} and an albedo of 0.23, resembling a grass crop of uniform height, well-watered, and growing actively. For annual crops, the stage of growth, as well as crop characteristics, affect the coefficients; thus, the k_c values must be growth stage-dependent. In the absence of a coupled crop-specific growth model, the transition to various stages depends on climatic factors; thus, the crop coefficients vary according to location as well as time. The *SWS* user manual presents length of crop stages for use in calculation of crop coefficients, crop coefficients for major crops, and selected locations and planting dates, all taken from *FAO Irrigation and Drainage Paper 56* (Allen et al. 1998).

Concentration/Production of Carbon Dioxide

Factors controlling soil carbon dioxide concentrations

The carbon dioxide concentration in the soil air is always elevated relative to the concentration in the earth's atmosphere. Carbon dioxide is produced in the soil primarily as a result of two processes: microbial respiration and root respiration from plants. The soil CO_2 concentration is dynamic with both seasonal changes and short-term changes. Changes in concentration are due to changes in production of CO_2 as well as changes in the transport rate of CO_2, which is mostly related to changes in the air-filled porosity of the soil but can also be related to the flow of water. In the rootzone and at some distance below it, the quantity of CO_2 added or removed by mineral dissolution/precipitation reactions is usually relatively small compared to the gas production and flux values and thus is neglected for simplification. A few meters below the rootzone, microbial respiration is greatly reduced, and mineral reactions may need to be considered in order to predict CO_2 gas concentration.

Carbon dioxide production. Šimůnek and Suarez (1993) described a general model for CO_2 production and transport that is included in the *SWS* model. The CO_2 production is represented as the sum of the production rate by soil microorganisms, γ_s [$cm^3\ cm^{-3}T^{-1}$], and the production rate by plant roots, γ_p [$cm^3cm^{-3}T^{-1}$]:

$$P = \gamma_s + \gamma_p = \gamma_{s0}\prod_i f_{si} + \gamma_{p0}\prod_i f_{pi} \qquad (28\text{-}23)$$

where the subscript s refers to soil microorganisms, and the subscript p refers to plant roots; ϑf_{si} is the overall reduction coefficient for microbial CO_2 production and is the product of reduction coefficients dependent on depth, temperature, pressure head (the soil water content), CO_2

concentration, and osmotic head. The term ϑf_{pi} is the overall reduction coefficient for plant root CO_2 production and is the product of reduction coefficients dependent on depth, temperature, pressure head (the soil water content), CO_2 concentration, osmotic head, and time. The parameters γ_{s0} and γ_{p0} represent, respectively, the optimal CO_2 production by the soil microorganisms or plant roots for the whole soil profile at 20 °C under optimal water, solute, and soil CO_2 concentration conditions [$cm^3cm^{-2}\ T^{-1}$]. The individual reduction functions are given in Šimůnek and Suarez (1993), and a discussion of selection of the values for optimal production, as well as coefficients for the reduction functions, is given in Suarez and Šimůnek (1993).

Carbon dioxide transport. The *SWS* model uses the one-dimensional CO_2 transport model presented by Šimůnek and Suarez (1993). The model considers CO_2 transport in the soil by both the liquid and gas phases. Thus, the CO_2 transport is described by convective transport in the aqueous phase and diffusive transport in both gas and aqueous phases, and by CO_2 production and/or removal. The one-dimensional CO_2 transport is described by

$$\frac{\partial c_T}{\partial t} = -\frac{\partial}{\partial z}(J_{da} + J_{dw} + J_{ca} + J_{cw}) - S_{c_w} + P \qquad (28\text{-}24)$$

where J_{da} is the CO_2 flux resulting from gas phase diffusion [cm d^{-1}], J_{dw} is the CO_2 flux resulting from dispersion in the dissolved phase [cm d^{-1}], J_{ca} the CO_2 flux caused by convection in the gas phase [cm d^{-1}], and J_{cw} the CO_2 flux caused by convection in the dissolved phase [cm d^{-1}]. The term c_T is the total volumetric concentration of CO_2 [cm^3cm^{-3}] and P is the CO_2 production/sink term [cm^3cm^{-3} d^{-1}]. The term Sc_w represents the dissolved CO_2 removed from the soil by root water uptake. This assumes that when plants take up water, the dissolved CO_2 is also removed from the soil-water system. Details of the production and transport routines are given in the user manual.

SOIL AND WATER CHEMISTRY

Transport

The governing equation for one-dimensional advective-dispersive chemical transport under transient flow conditions in partially saturated porous media is taken as (Suarez and Šimůnek 1992):

$$\frac{\partial \theta c_{ri}}{\partial t} + \rho \frac{\partial \bar{c}_{ri}}{\partial t} + \rho \frac{\partial \hat{c}_{ri}}{\partial t} = \frac{\partial}{\partial z}\left[\theta D \frac{\partial c_{ri}}{\partial z} - q c_{ri}\right] \quad i = 1, n_s \qquad (28\text{-}25)$$

where c_{Ti} is the total dissolved concentration of the aqueous component i [ML^{-3}], $\bar{c}_{Ti}$ is the total adsorbed or exchangeable concentration of the aqueous component i [Mkg^{-1}], $\hat{c}_{Ti}$ is the nonadsorbed solid-phase concentration of aqueous component i [Mkg^{-1}], ρ is the bulk density of the soil [ML^{-3}], D is the dispersion coefficient [$cm^2\ d^{-1}$], q is the volumetric flux [$cm\ d^{-1}$], and n_s is the number of aqueous components. The second and third terms on the left side of Eq. 28-25 are zero for components that do not undergo ion exchange, adsorption, or precipitation/dissolution. The coefficient D is the sum of the diffusion and dispersion components:

$$D = \tau D_m + \lambda \frac{|q|}{\theta} \tag{28-26}$$

where τ is the tortuosity factor, D_m is the coefficient of molecular diffusion [$cm^2\ d^{-1}$], and λ is the dispersivity [cm]. This equation is a simplified treatment of the diffusion process. A more detailed description of the diffusion process requires calculation of the diffusion rates of individual species requiring coupling of individual ion fluxes to the concentration gradients of all individual species. This simplification appears justified since, in soils, errors generated by uncertainty in determination of the tortuosity factor and velocity vectors are more significant for solute transport than errors associated with this treatment of diffusion.

Chemical Model

The chemical model includes consideration of nine major aqueous components, consisting of Ca, Mg, Na, K, SO_4, Cl, alkalinity, NO_3 and B. Alkalinity is defined as

$$\begin{aligned}\text{Alkalinity} = {} & [HCO_3^-] + 2[CO_3^{2-}] + 2[CaCO_3^0] + \\ & [CaHCO_3^+] + 2[MgCO_3^0] + [MgHCO_3^+] + 2[NaCO_3^-] + \\ & [NaHCO_3^0] + [B(OH)_4^-] - [H^+] + [OH^-]\end{aligned} \tag{28-27}$$

where brackets represent concentrations (mol kg−1). From these components we obtain 11 primary species: Ca^{2+}, Mg^{2+}, Na^+, K^+, SO_4^{2-}, Cl^-, HCO_3^-, CO_3^{2-}, NO_3^-, $B(OH)_4^-$ and H_3BO_3. In addition, we include the ion pair/complexes $CaHCO_3^+$, $CaCO_3^0$, $CaSO_4^0$, $MgHCO_3^+$, $MgCO_3^0$, $MgSO_4^0$, $NaHCO_3^0$, $NaCO_3^-$, $NaSO_4^-$, and KSO_4^-. Alkalinity as defined in Eq. 28-27 is a conservative quantity, affected only by dissolution or precipitation of a carbonate phase (such as calcite).

After calculation of the soil air phase CO_2 partial pressure (from the production and transport routines or from the user specified input),

$H_2CO_3^*$ (sum of aqueous CO_2 and H_2CO_3) is calculated using a Henry's Law expression:

$$k_{CO_2} = \frac{(H_2CO_3^*)}{P_{CO_2}(H_2O)} \tag{28-28}$$

where P_{CO_2} is the partial pressure of CO_2 (atm.), and parentheses denote activities. From the $H_2CO_3^*$ value and utilizing the equations for the first and second dissociation constants of carbonic acid, conservation of mass, and the equations for dissociation of the complexes, we solve the equations using an iterative approach. The soil solution pH is determined as a dependent variable from solution of Eq. 28-27 for $[H^+]$ and the activity coefficient. All equilibrium constants are calculated from available temperature-dependent expressions. Soil temperature is calculated from a heat flow submodel, with input of air temperature data and the initial soil temperature profile.

Osmotic pressure

The osmotic pressure is used to calculate the impact of salinity on water uptake and plant yield. Osmotic pressure is calculated from

$$P_\varphi = RT\frac{M_s v m \varphi}{V_s m^0} \tag{28-29}$$

where P_φ (Pa) is the osmotic pressure of the solution, R is the gas constant, T is absolute temperature, V_s is the partial molar volume of the water, m^0 is unit molality, m is molality of the solution, φ is the osmotic coefficient of the solution, and M is the molar weight (Stokes 1979) . The osmotic pressure in Pa is converted to osmotic pressure in m by the expression

$$h_\varphi = \frac{P_\varphi}{\rho g} \tag{28-30}$$

The osmotic coefficient is calculated from Pitzer (1973). Detail is provided in the user manual.

Activity coefficients

Activity coefficients in the *SWS* model are determined by default using an extended version of the Debye-Huckel equation (Truesdell and Jones 1974):

$$\ln\gamma = -\frac{Az^2\sqrt{I}}{1 + Ba\sqrt{I}} + bI \tag{28-31}$$

where A and B are constants depending on the dielectric constant of water, density, and temperature; z is the ionic charge; a and b are adjustable ion parameters; and I is the ionic strength. At higher ionic strength (>0.3 M), the solution is sufficiently concentrated that all ion interactions must be considered for calculation of activity coefficients. In this instance, the Pitzer expressions are utilized. The activity coefficients are expressed in a virial-type expansion having the form (Pitzer 1979)

$$\ln \gamma_i = \ln \gamma_i^{DH} + \sum_j B_{ij}(I) m_j + \sum_j \sum_k C_{ijk} m_j m_k + \cdots \qquad (28\text{-}32)$$

where γ_i^{DH} is a modified Debye-Huckel activity coefficient and B_{ij} and C_{ij} are coefficients specific to each ion interaction. The Pitzer approach considers ion–ion interactions for every species in solution; thus, it does not consider the individual ion pairs and complexes, such as $NaSO_4^-$ described above as a species when using the extended Debye-Huckel equation and ion association model. The Pitzer model is considered suitable for prediction of species activity in solutions up to 20 mol kg^{-1}, a concentration well above the intended use of the *SWS* model.

Solid phases

Because the model considers a restricted set of solid phases, it cannot be used to predict the composition of a brine undergoing evaporation. The minerals considered include calcite, gypsum, hydromagnesite, nesquehonite, and sepiolite. Since the model attempts to predict water composition, it cannot be based only on thermodynamic considerations. Dolomite precipitation is not considered by the present model because ordered dolomite has not been observed at near-earth surface conditions. The kinetics of dissolution are also sufficiently slow that it is not reasonable to assume that a solution is dolomite-saturated merely because dolomite is present in the soil profile. It is beyond the scope of this model to consider the detail necessary for a kinetic description of dolomite dissolution. This omission is significant only if dolomite is present and calcite is not. The model tracks all changes in the quantities of the solid phases due to precipitation or dissolution.

Calcite precipitation

The equilibrium condition of a solution saturated with calcite in the presence of CO_2 can be described by the expression

$$(Ca^{2+})(HCO_3^-)^2 = \frac{K_{sp}^C K_{CO_2} K_{a_1}}{K_{a_2}} P_{CO_2}(H_2O) = K_{sp}^C K_r \qquad (28\text{-}33)$$

where parentheses denote activities, K_{CO_2} is the Henry's Law constant for the solubility of CO_2 in water, K_{a_1} and K_{a_2} are the first and second dissociation constants of carbonic acid in water, and K_{SP}^{C} is the solubility product for calcite. To obtain equilibrium [i.e., when the ion activity product (IAP) is equal to the solubility product K_{sp}], a quantity x of Ca^{2+} and HCO_3^- must be added or removed from the solution (right-hand side of Eq. 28-33) to satisfy the equilibrium condition.

It has been shown that waters below irrigated regions are supersaturated with respect to calcite, and the average IAP can be represented by $10^{-8.0}$ (Suarez 1977; Suarez et al. 1992)—a value about three times greater than that predicted by calcite equilibrium. Thus, the equilibrium condition significantly underestimates the Ca solubility in soil solutions. The cause of supersaturation has been shown to be due to poisoning of crystal surfaces by dissolved organic matter (Inskeep and Bloom 1986; Lebron and Suarez 1996). For the purposes of the *SWS* model, the nucleation rate is sufficiently fast, and the crystal growth rate sufficiently slow, that the calcite solubility can be taken at the point of supersaturation at which there is no further nucleation. This level of supersaturation is significantly close to the supersaturation with respect to calcite observed in field measurements. The model thus uses the apparent solubility of 1.0×10^{-8}, with the temperature dependence determined for calcite. This is not an equilibrium value, but it is the suitable value to simulate calcium carbonate solubility in the soil zone.

Gypsum

The model allows the user to specify the initial presence of gypsum, requiring input of the quantity present. If gypsum is present in any soil layer at the given time step, the model forces the solution to gypsum equilibrium. The program tracks changes in the amount of gypsum present if all gypsum is dissolved in a soil layer, such as during reclamation of a sodic soil, in which case gypsum equilibrium is no longer forced. In all cases, gypsum precipitates wherever supersaturation is indicated by solution calculations. For the objectives of this model, it is reasonable to assume that the kinetics of gypsum dissolution/precipitation are sufficiently fast that the equilibrium condition can be used.

Magnesium precipitation

The model considers that Mg precipitation can occur as a carbonate (either nesquehonite or hydromagnesite), or as a silicate (sepiolite). Since this is a predictive model, it considers only phases that either precipitate under earth surface conditions or occur frequently and are reactive under earth surface conditions; these need not necessarily be the thermodynam-

tically most stable. With this consideration, magnesite is neglected because it apparently does not form under earth surface temperatures, is relatively rare, and its dissolution rate is exceedingly small, such that its solubility has not yet been satisfactorily determined from dissolution studies at or near 25 °C. Similarly, dolomite precipitation is not considered, because true dolomite appears to form very rarely in soil environments.

If nesquehonite or hydromagnesite saturation is reached, the model will precipitate the predicted Mg carbonate. The Mg carbonate precipitated, combined with calcite precipitation, will likely represent the mixed Ca-Mg precipitate that is observed in hypersaline environments, often called protodolomite (sometimes incorrectly called dolomite). However, the resulting solution composition is much different from that produced by simply forcing equilibrium with respect to dolomite, as the model forms this mixed precipitate (calcite + hydrated magnesium carbonate) under conditions of high supersaturation with respect to dolomite. This result is consistent with the high levels of dolomite supersaturation maintained in high-Mg waters. Precipitation (or dissolution, if present in the soil) of sepiolite is also considered by the model. Sepiolite will readily precipitate into a solid with a K_{SP}^{S} greater than that of well-crystallized sepiolite. Formation of this mineral requires high pH, high Mg concentrations, and low CO_2 partial pressure.

Cation Exchange

Cation exchange is generally the dominant chemical process for the major cations in solution in the unsaturated zone. Generally, cation exchange is treated with a Gapon-type expression of the form (White and Zelazny 1986)

$$K_{ij} = \frac{\overline{c}_i^{y+}}{\overline{c}_j^{x+}} \frac{(c_j^{x+})^{1/x}}{(c_i^{y+})^{1/y}} \tag{28-34}$$

where y and x are the valences of species i and j, respectively, and the overscored concentrations are those of the exchange phase (expressed in $mol_c\ mass^{-1}$). It is assumed that the cation exchange capacity c_T is constant, and for nonacid soils

$$\overline{c}_T = \overline{Ca}^{2+} + \overline{Mg}^{2+} + \overline{Na}^{+} + \overline{K}^{+} \tag{28-35}$$

Experimentally determined selectivity values for a given cation pair are not constant over the full range of composition. In addition, the cation exchange capacity (CEC) varies as a function of pH due to variable charge materials such as organic matter. It has been observed that soils have an

increased preference for Ca^{2+} over Na^{+}, and Ca^{2+} over Mg^{+}, at low levels of exchange phase Ca^{2+}. Suarez and Wood (1993) developed a mixing model used in *UNSATCHEM* (Suarez and Šimůnek 1997) that is able to approximate the nonconstant values of the soil selectivity coefficient by taking into account the organic matter content of the soil and using the published constant selectivity values for clay and organic matter. Calcium preference decreases as the organic matter exchange sites (which have higher Ca preference than clays) become Ca saturated. This approach is useful to predict the input exchange constants if the selectivity values of the soil are not known and if substantial organic matter is present. This option is not directly available in the *SWS* model interface but can be applied by the user via the input file using a standard file editor. The model has default exchange selectivity values, but the user should specify soil-specific values if available.

Boron

The major chemical process affecting B concentration and transport in soils is adsorption. Various adsorption models are available, but the constant capacitance model (CCM; Herbelin and Westall 1996) has been demonstrated to well-represent B adsorption with soils (Goldberg and Glaubig 1986; Goldberg et al. 2000). Application of chemical complexation models into transport models has been hampered primarily by the need to have the soil-specific characterization and model parameters, requiring time-consuming laboratory studies. When fitting the CCM model to experimental data, Goldberg et al. (2000) found that a good fit to the CCM model was obtained by selecting the surface species as $SH_3BO_4^-$; the surface reaction was written as

$$SOH + H_3BO_3 \leftrightarrow SH_3BO_4^- + H^+ \tag{28-36}$$

The intrinsic equilibrium constants are given as

$$K_{+} = \frac{[SOH_2^+]}{[SOH][H^+]}\exp(F\psi/RT) \tag{28-37}$$

$$K_{-} = \frac{[SO^-][H^+]}{[SOH]}\exp(-F\psi/RT) \tag{28-38}$$

$$K_{B-} = \frac{[SH_3BO_4^-][H^+]}{[SOH][H_3BO_3]}\exp(-F\psi/RT) \tag{28-39}$$

where F is the Faraday constant (C $mol_c L^{-1}$), ψ is the surface potential (V), R is the molar gas constant, T is the absolute temperature (K), and brackets indicate concentrations in mol L^{-1} (Goldberg et al. 2000).

Goldberg et al. (2000) developed regression equations for the prediction of the three CCM surface complexation constants based on generally available soil properties. The following equations were developed:

$$LogK_{B-} = -9.14 - 0.375\ln(SA) + 0.167\ln(OC) + 0.11\ln(IOC) + 0.466\ln(Al) \quad (28\text{-}40)$$

$$LogK_{+} = 7.85 - 0.102\ln(OC) - 0.198\ln(IOC) - 0.622\ln(Al) \quad (28\text{-}41)$$

$$LogK_{-} = -11.97 + 0.302\ln(OC) + 0.0584\ln(IOC) + 0.302\ln(Al) \quad (28\text{-}42)$$

where SA is the surface area, measured by ethylene glycol monoethyl ether (EGME); OC is the organic carbon; IOC is the inorganic carbon; and Al is the extractable Al (including absorbed and reactive hydroxides and oxides). Using these relationships, Goldberg et al. (2000) predicted the absorption envelopes (adsorption as a function of pH) for a series of arid land soils. They concluded that the fits using the CCM with the constants determined from the stated predictive equations were acceptable for use in modeling adsorption. These constants have been added to the *SWS* model along with a routine to solve the CCM equations, enabling soil-specific prediction of B adsorption and transport as related to soil properties and solution pH.

SWS APPLICATIONS

This section describes several published applications and utilizations of the model or incorporated routines. The capabilities to predict changes in water content, CO_2 concentration, and leaching of salts and sodium during reclamation are demonstrated. Also presented are several examples of model simulations useful for water managers and engineers.

Prediction of Variable Water Content and CO_2

Suarez and Šimůnek (1993) utilized field data published by Buyanovsky and Wagner (1983). This field data set is relatively unusual in that it presents detailed information about the extent and timing of rain events, average air temperature, and the changes in water content and CO_2 throughout a period of almost 1 year. The simulation used the described soil

properties, including texture, organic matter, and air porosity at field capacity, but the available data set did not contain detailed hydraulic information. The data set input to the model was thus limited to the soil properties, rooting depth, rain events and quantities, average air temperature, and ET_0 estimates. These inputs represent a level of information that would be realistic for management decisions. As shown in Fig. 28-1, there was a good correspondence between the measured water content at 0.2 m and the model-simulated water content. Similarly, Fig. 28-2 shows that the model was well able to predict the field CO_2 concentrations (Suarez and Šimůnek 1993), over a range of conditions, including those where transport (under winter conditions and low water content) and CO_2 production (warm conditions) predictions could be evaluated.

Saline Sodic Soil Reclamation: Model Versus Field Data

Suarez (2001) examined the reclamation of a saline sodic field and compared the field results to predictions using *UNSATCHEM* 3.1 (Suarez and Šimůnek 1997). The 40-ha field was mapped for salinity using an electromagnetic (Geonics EM-38) unit. Soil samples (24 cores sampled in 30-cm intervals) were also collected before and after reclamation based on the EM map to capture the field variability. Shown in Figs. 28-3 and 28-4 [after Suarez (2001)] are the initial and final median EC and SAR values as a function of depth. A total of 114 cm of water was applied to the field

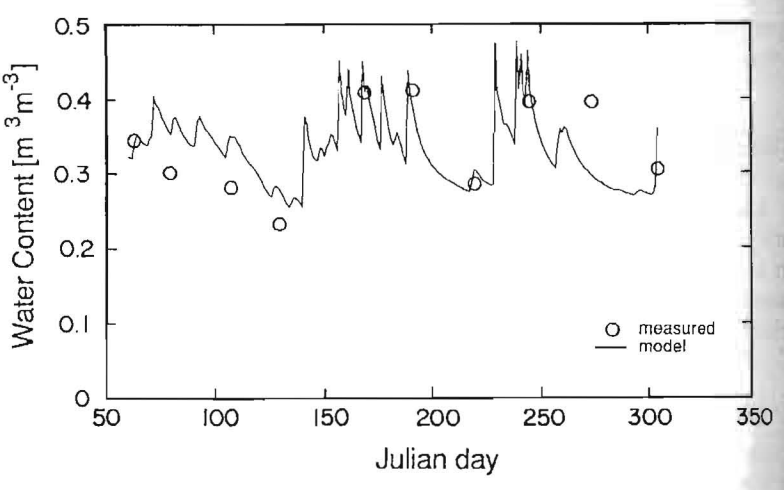

FIGURE 28-1. Measured (Buyanovsky and Wagner 1983) and calculated water contents at a depth of 0.20 m for a Missouri wheat experiment, 1982. From Suarez and Šimůnek (1993).

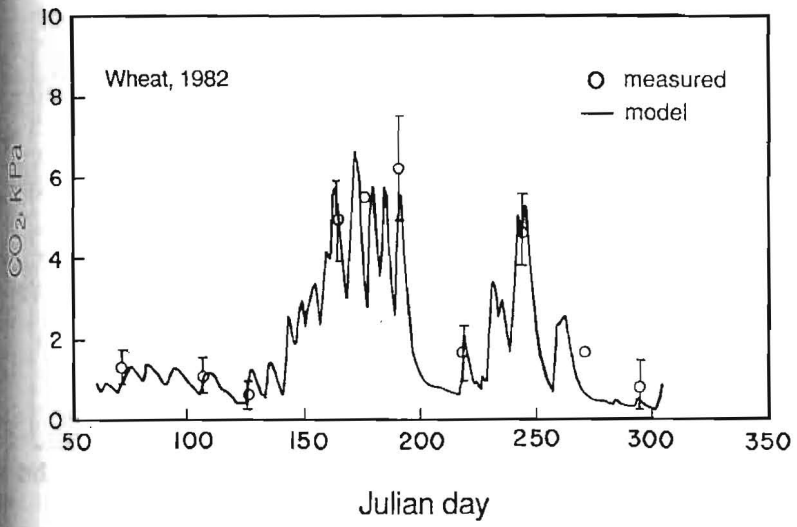

FIGURE 28-2. Measured (Buyanovsky and Wagner 1983) and calculated CO_2 concentrations at a depth of 0.20 m for a Missouri wheat experiment, 1982. Vertical bars show standard deviations. From Suarez and Šimůnek (1993).

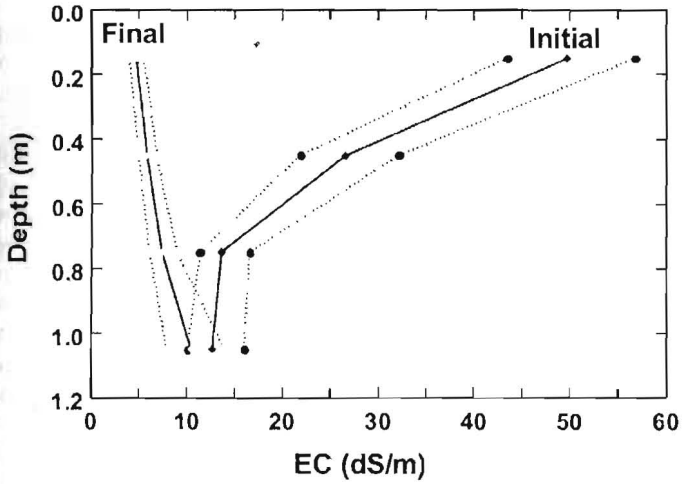

FIGURE 28-3. Median EC values with depth for both initial and final (after leaching) conditions. Reclamation consisted of application of 24 Mg/ha of gypsum and application of 114 cm of water. The dashed lines indicate the 95% confidence limits of the median for the field. From Suarez (2001).

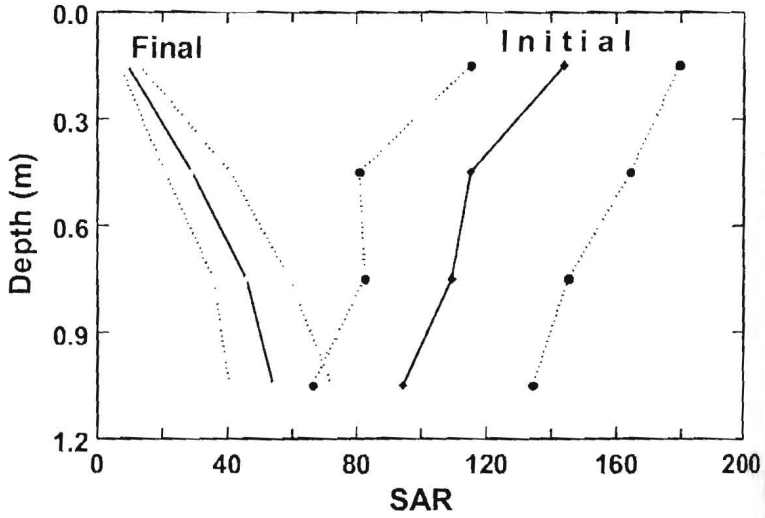

FIGURE 28-4. Median SAR values with depth for both initial and final (after leaching) conditions. Reclamation consisted of application of 24 Mg/ha of gypsum and application of 114 cm of water. The dashed lines indicate the 95% confidence limits of the median for the field. From Suarez (2001).

(ponded) along with incorporation of 24 Mg/ha of gypsum to a depth of 15 cm. Based on climatic data for the time interval during the ponding event, it was calculated that only 74 cm infiltrated, with 40 cm of surface evaporation.

The model simulation used only the initial soil profiles, water applied (volume and EC), initial soil saturation extract EC and SAR, soil texture (used to estimate hydraulic parameters), estimated soil CEC (based on mineralogy and texture), and quantity and depth of gypsum applied. As shown in Figs. 28-5 and 28-6, both the EC profile and the change in SAR were satisfactorily predicted with the correct amount of water. Note that the model was not "calibrated" by adjusting parameters, nor was the input modified, demonstrating that a deterministic transient model can give useful results for a field application without excessive input data.

Optimizing Reclamation Using *SWS*

When reclaiming a sodic field, many options are available. Although a model prediction cannot be used alone to select the best option, it can be used as part of the decision-making process. The following examples are from Suarez (2001). Deeper placement of gypsum increases costs of soil

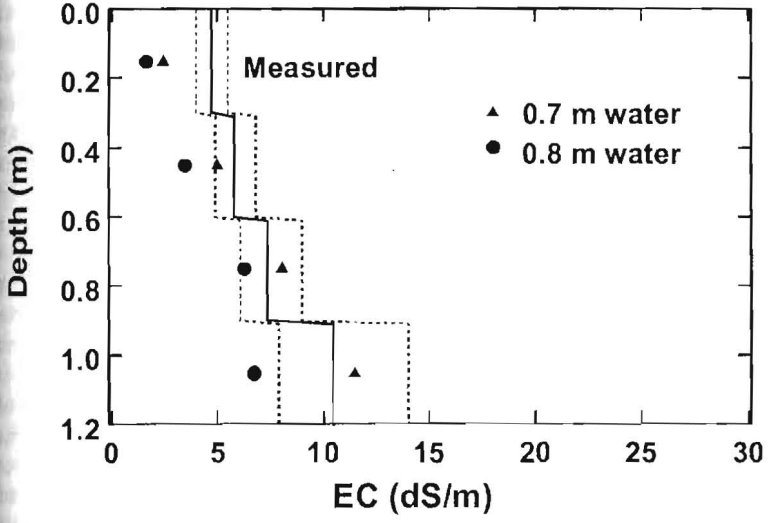

FIGURE 28-5. Comparison of measured and model predicted changes in EC with depth after mixing 24 Mg/ha of gypsum into the top 15 cm and then infiltration of 70 and 80 cm of water. From Suarez (2001).

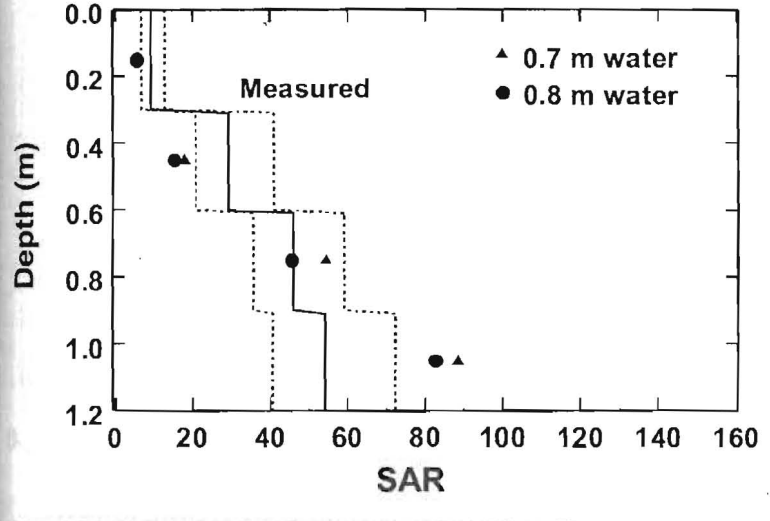

FIGURE 28-6. Comparison of measured and model predicted changes in SAR with depth after mixing 24 Mg/ha of gypsum into the top 15 cm and then infiltration of 70 and 80 cm of water. From Suarez (2001).

soil reclamation but may result in use of less water. Shown in Fig. 28-7 is a comparison of the relative effectiveness of reclamation as related to depth of gypsum incorporation (equal quantities of gypsum). As shown, shallow placement of gypsum (top 2 cm) will not reclaim this field adequately with 80 cm of water. Additional water (and thus time) is required to reclaim to the same extent as predicted for deeper placement. This is due to the fact that gypsum solubility is enhanced in the presence of high exchangeable Na, so that the gypsum dissolves with less water if it is incorporated deeper in the profile.

The optimal placement depth of gypsum depends on several factors. Deep placement of gypsum is more expensive and will enable reclamation to a greater depth, but, depending on the quantity used, it may not adequately reclaim the important top 15 cm. Based on Fig. 28-7, it can be concluded that for this site and the amount of gypsum and water used, 8- to 15-cm placement of the gypsum is sufficiently deep. The optimal depth of placement and quantity of gypsum to apply will thus depend on the depth needed to be reclaimed, initial exchangeable sodium percentage, CEC, cost and availability of water, and cost of gypsum incorporation The *SWS* model is suited to predict various scenarios and enable the user to decide the optimal practice for the specific site. For example, gypsum placement on the surface or in the water may be less expensive than

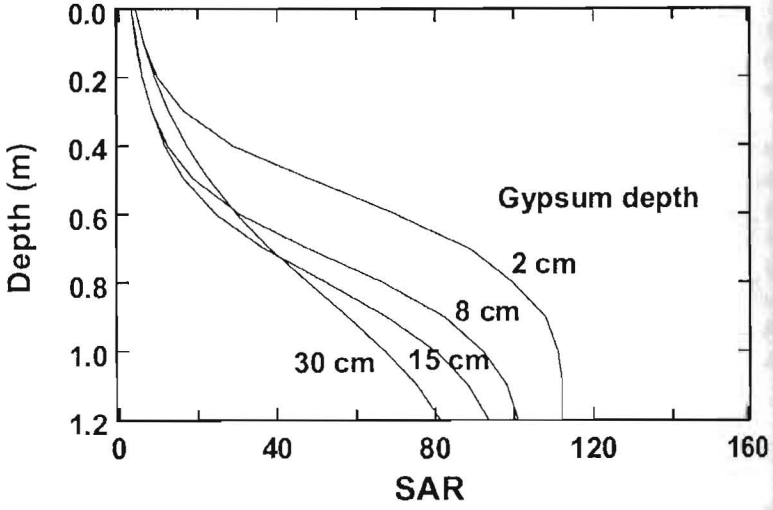

FIGURE 28-7. Comparison of model-predicted changes in SAR with depth after mixing 24 Mg/ha gypsum into the top 2, 8, 15, and 30 cm of soil and leaching with 80 cm of water. From Suarez (2001).

incorporating into the soil, but it will require more time and larger quantities of water.

An alternative or complement to gypsum reclamation for calcareous soils is enhancement of the CO_2 concentration in the soil air and reclamation by dissolution of calcite. The concept of green manuring as a sodic reclamation practice has been discussed and applied with mixed results. Shown in Fig. 28-8 are simulations with a CO_2 partial pressure of 5 kPa, comparable to what could be achieved by incorporating organic matter and flooding the soil under warm soil conditions. Although less effective than gypsum, use of the calcite in the soil can nonetheless reduce the quantity of gypsum and can sometimes avoid the entire cost of gypsum and its application. In a calcareous soil, calcite dissolution and its reclamation effect should be considered when determining gypsum requirements.

The disadvantage of using the soil calcite alone for sodic soil reclamation, as compared with gypsum, is that it requires more water to achieve the same final SAR in the soil. This is shown in Fig. 28-8 compared to Fig. 28-7. As shown in Fig. 28-9 (Suarez 2001), up to 32 $mmol_c/L$ of alkalinity may be released when reclaiming a sodic soil using calcite and green manuring. This indicates that calcite, in combination with cation exchange, can release an amount of Ca comparable to that released from gypsum

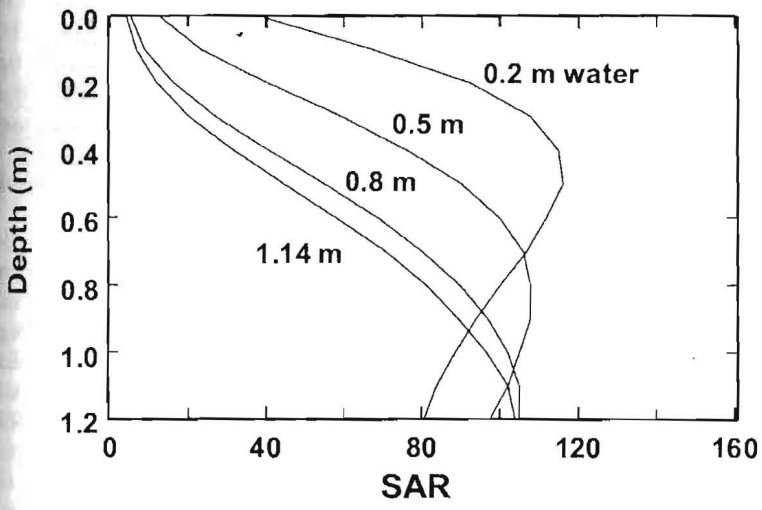

FIGURE 28-8. Model-predicted changes in SAR with depth after elevating the CO_2 to 5 kPa in the presence of calcite, then leaching with 20, 50, 80, and 114 cm of water. From Suarez (2001).

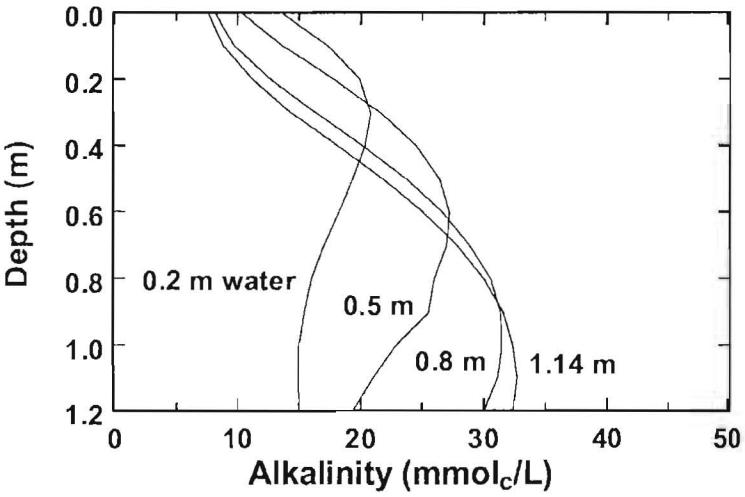

FIGURE 28-9. Model-predicted alkalinity concentrations (mmol$_c$/L) with depth after elevating the CO_2 to 5 kPa in the presence of calcite, and then leaching with 20, 50, 80, and 114 cm of water. From Suarez (2001).

placement on the surface. Under cold soil conditions, the model predicts that the CO_2 production is reduced and very large quantities of water are required. The model can also be used to examine the interaction of EC, SAR, and hydraulic relationships to ensure that the EC does not drop rapidly and cause soil dispersion before the SAR is reduced to a safe level. Based on the simulation, green manuring will fail when insufficient calcite is present, the initial EC is not sufficiently high for the initial SAR to prevent dispersion or swelling, or CO_2 production is inadequate (cold conditions).

The hazard to water supplies receiving drainage water from a sodic soil reclamation project must also be considered. As discussed previously, up to 32 mmol$_c$/L of alkalinity may be released when reclaiming a calcareous sodic soil using green manuring. In this instance the drainage water would be of very high pH (>9.0) once it degasses, with high alkalinity and low Ca concentration. Reclamation with gypsum will also increase the salt load of discharging waters, in this instance primarily sodium sulfate.

Effect of Rain on Sodium Adsorption Ratio

Shown in Fig. 28-10 are the soil EC profiles after 1 to 5 cm of rain infiltrated into a loam soil (Suarez et al. 2006). These simulations are for cal-

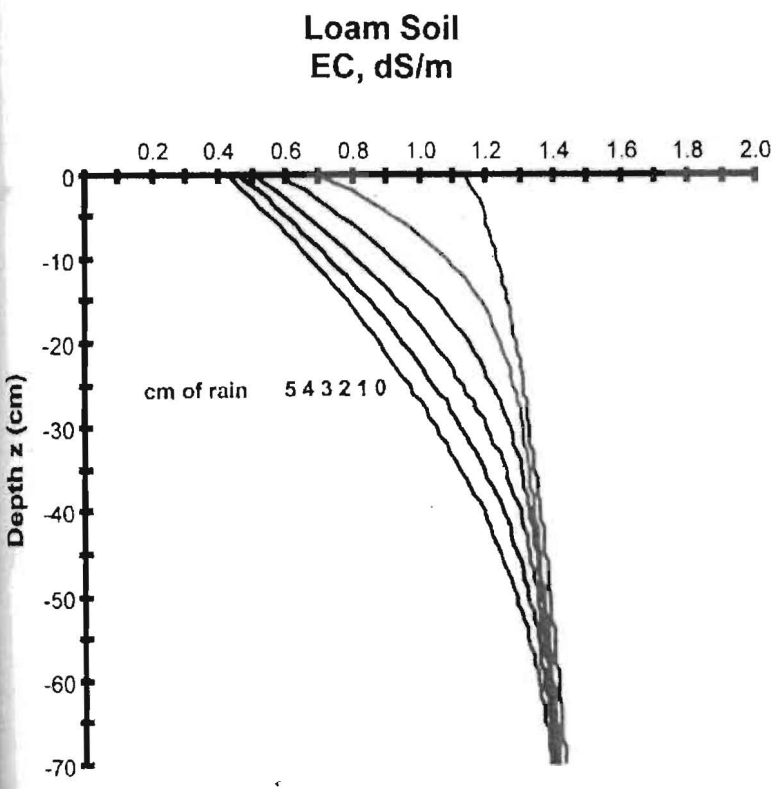

FIGURE 28-10. Predicted relationship of EC with depth and quantity of rain infiltrated for Glendive loam soil. The initial condition was EC = 1.0 dS/m and SAR = 10. Each curve represents addition of 1 cm of rain. From Suarez et al. (2006).

areous soils first irrigated with water of EC = 1.0 dS/m and SAR = 10. The initial soil EC is higher than the input irrigation water EC and it increases with depth due to predicted calcite dissolution in the soil. The simulation input included the measured soil CEC. As shown, the predicted EC at the surface decreased during the rain event, decreasing to 0.42 dS m^{-1} at the surface after infiltration of 5 cm of rain. Calcite dissolution during the rain event is enhanced by the exchange of solution Ca for Na on the clay exchange sites, thus causing a reduction in the SAR with time, as shown in Fig. 28-11. The SAR was still equal to 5.5 at the surface after 5 cm of rain. The decrease in SAR was not sufficient to compensate for the decrease in EC; thus, the simulation shows that the sodium hazard is increased during the rain event. A surface treatment (such as gypsum)

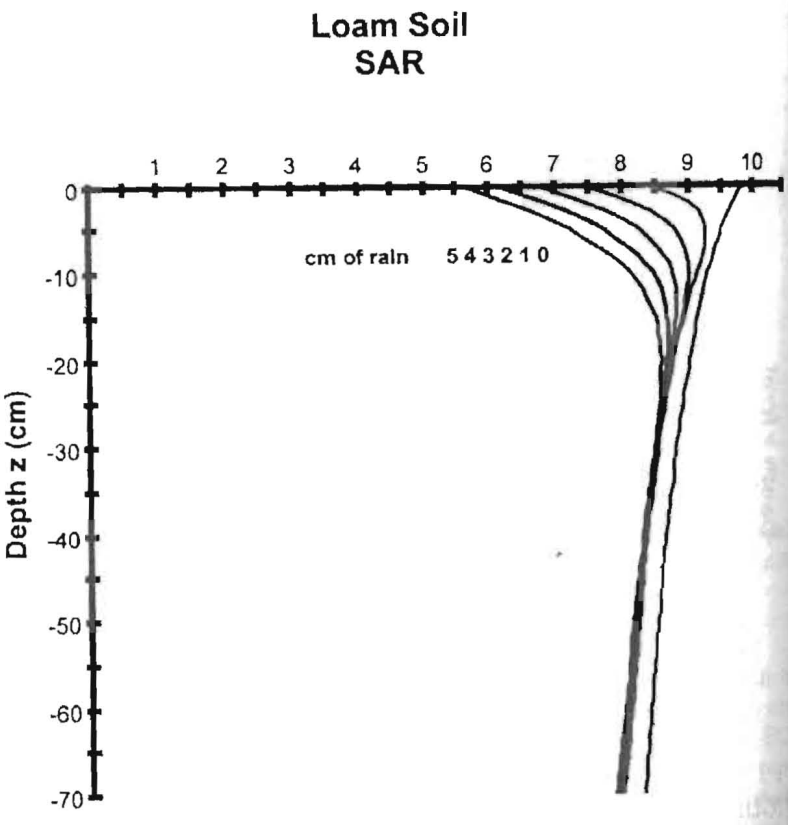

FIGURE 28-11. Predicted relationship of SAR with depth and quantity of rain infiltrated. The initial condition was EC = 1.0 dS/m and SAR = 10. Each curve represents addition of 1 cm of rain. From Suarez et al. (2006).

is likely needed if there is substantial rain on this soil when it is also irrigated with water of SAR = 10 and EC = 1 dS m^{-1}.

The predicted change in EC and SAR for rain on a clay soil irrigated with the same water is shown in Figs. 28-12 and 28-13, respectively (Suarez et al. 2006). The decrease in EC at the surface is similar to but slightly less than that observed for the loam soil (Fig. 28-10). This difference is caused by the increased dissolution of calcite due, in turn, to the increased cation exchange of the clay soil. As shown in Fig. 28-13, the SAR of the clay soil was buffered, and there was only a small SAR reduction after infiltration of 5 cm of rain. The high CEC of the clay soil allows the soil exchange sites to buffer the solution SAR. The soil surface of the clay soil at the end of the

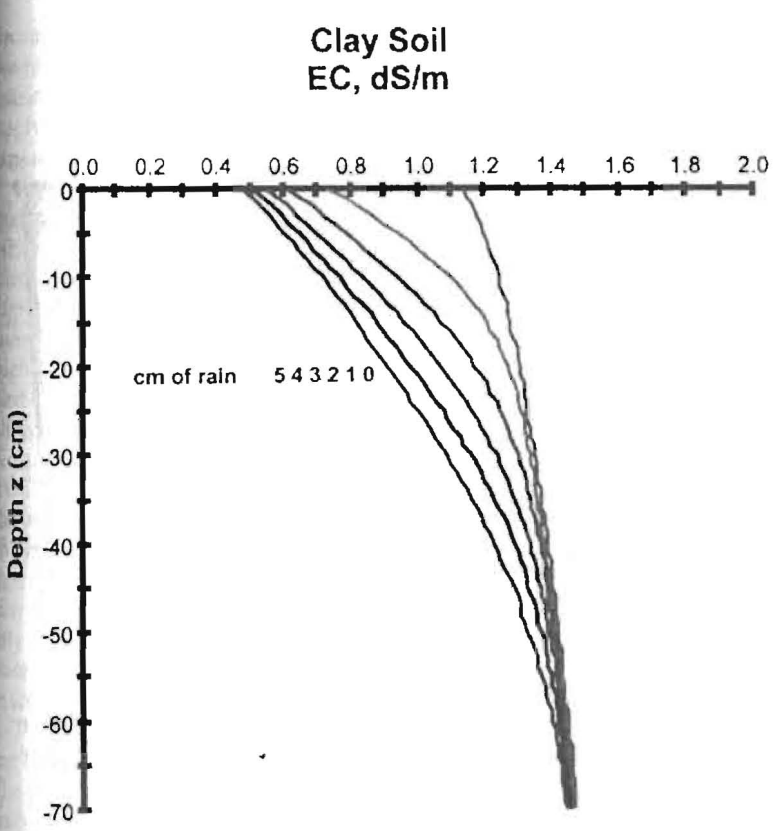

FIGURE 28-12. Predicted relationship of EC with depth and quantity of rain infiltrated into the clay soil. The initial condition was EC = 1.0 dS/m and SAR = 10. Each curve represents addition of 1 cm of rain. From Suarez et al. (2006).

rain event is thus at low EC with almost no decrease in SAR relative to the pre-rain condition. These simulations suggest that the chemical effects related to the infiltration hazard of rain or irrigation waters of low salinity on a sodic soil would be greater for soils of greater CEC. The model provides the temporal changes during the irrigation season and allows for simulation of different applications and timing of surface amendments.

Management of High-Boron Waters Used for Irrigation

Waters with B concentrations above 1 mg L^{-1} can be potentially toxic to B-sensitive crops, and almost all crops are adversely affected when

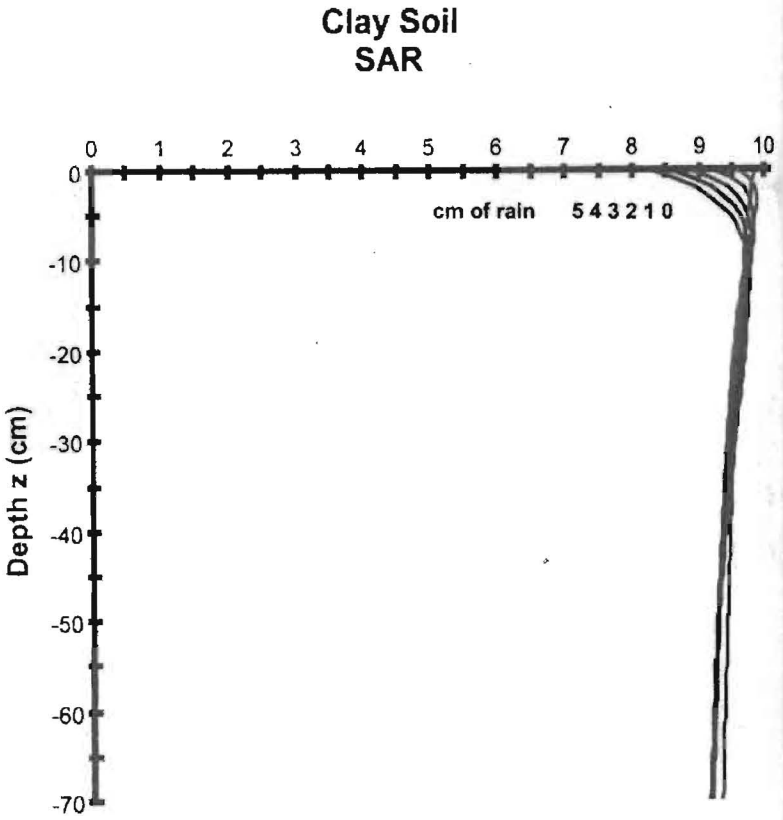

FIGURE 28-13. Relationship of SAR with depth and quantity of rain infiltrated into clay soil. The initial condition was SAR = 10. Each curve represents addition of 1 cm of rain. From Suarez et al. (2006).

concentrations in the soil water exceed 10 mg L^{-1}. The *SWS* simulations below demonstrate how the model can be used as a management tool when using low-quality waters for irrigation. Irrigation drainage water from Westside of the Central Valley in California typically has a B concentration of 4 to 8 mg L^{-1} and an EC of 8 to 14 dS m^{-1}. These waters are typically considered unusable for irrigation, or, if usable, then only with salt- and B-tolerant crops. With the traditional steady-state approach (in this case no adsorption-desorption), the B concentration is increased in the soil proportionally with the Cl concentration. Therefore, the traditional

recommendation when irrigating with high-B water is to increase the leaching fraction to maintain a lower B concentration in the rootzone. The subsequent model simulations examine two leaching regimes when applying a high-B concentration irrigation water on an initially low-B-containing soil.

The irrigation water used in the simulations contained a B concentration of 0.8 mmol L^{-1} (10 mg L^{-1}), considered to be unusable by all criteria. Although low-quality water is often not usable for sustained agricultural production, it can be utilized either by blending or cyclic use of low- and high-quality water. A steady-state model can adequately consider this by using the average B concentration. However, in a drought condition no high-quality water may be available, or it may be available only during part of the season. The soil profile was initially free of B. In the simulation shown in Fig. 28-14 (Goldberg and Suarez 2006), the ET was 1 cm/day with irrigation applications corresponding to an average input of 2 cm/day (leaching fraction of 0.5). A total of 200 cm of water was applied during the 100-day growing season. The surface area of 100 m^2 g^{-1} soil corresponded to a soil with relatively low B adsorption capacity, while that at 1,000 m^2 g^{-1} was a soil with high adsorption capacity. The irrigation of the low-adsorption-capacity soil caused the B concentration to rapidly increase to toxic levels (with concentrations approaching the steady-state values), while the higher-adsorbing soil was able to maintain the B in solution below that of the irrigation water.

The results of irrigating the same soils with the same waters at a leaching fraction of 0.1 are shown in Fig. 28-15 (Goldberg and Suarez 2006). The low-adsorbing soil had B concentrations increasing to higher levels with low leaching as compared to high leaching. The high-adsorbing soil saw relatively low concentrations of B, even after 100 days; at this time the B front is just reaching 25 cm. The mean rootzone B concentrations as a function of time are shown in Fig. 28-16 for the four simulations (Goldberg and Suarez 2006). The conclusions are that for a soil with high B adsorption capacity, there is little B hazard during the first year of cropping, and it is best to use low leaching fractions to minimize the B concentration and accumulation. At steady state, the lower leaching would eventually result in proportionally higher B concentrations than the more leached soil. For the low-B-adsorbing soil, the recommendation would be to use low leaching for 70 days and then switch to high leaching to prevent further B accumulation. These recommendations are opposite to recommendations based on the steady-state analysis. The mean B concentration in the rootzone is sufficiently low that many crops could be grown without yield loss. Sustained management would clearly require a better water source, either winter rains or leaching with higher-quality water, in the subsequent crop cycle.

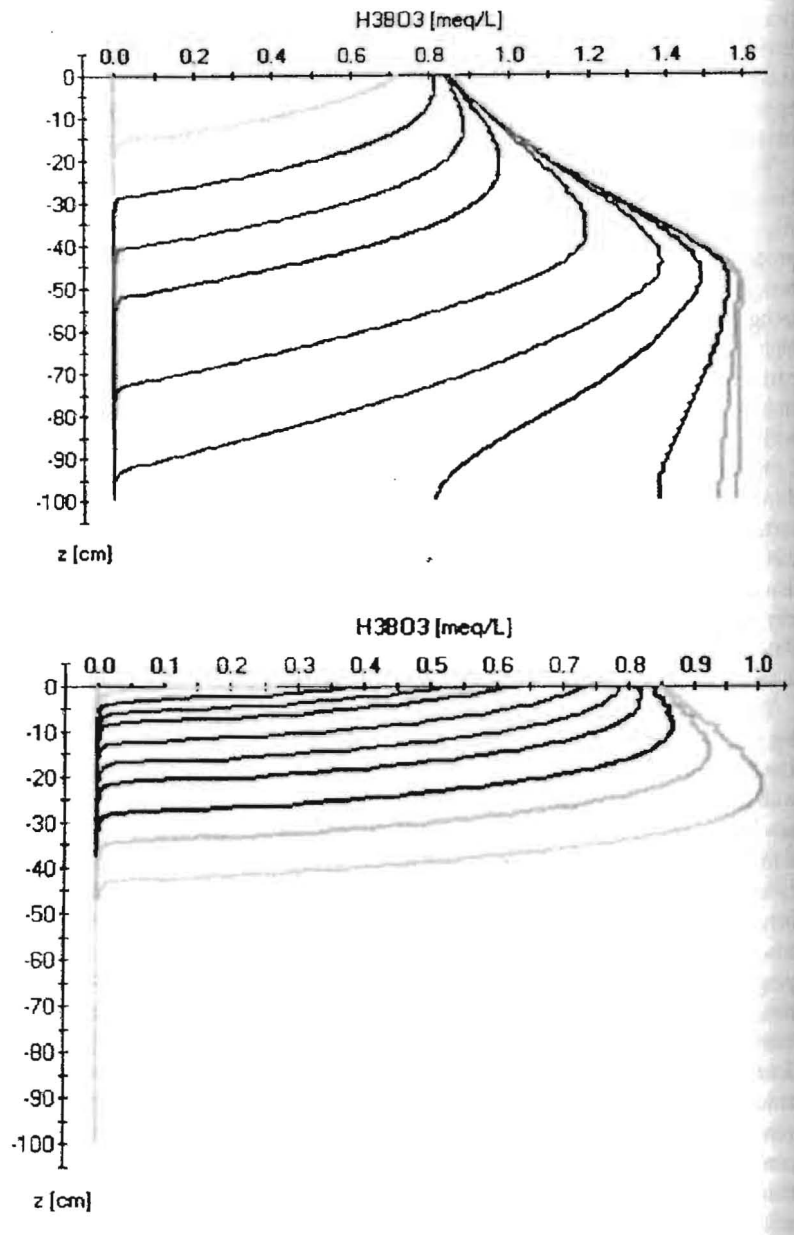

FIGURE 28-14. Change in boron concentration with depth and time (0, 10, 20, 30, 40, 50, 60, 70, 80, 90, and 100 days) for leaching fraction of 0.5 and soil surface area of (a) 100 m^2g^{-1}, and (b) 1,000 m^2g^{-1}. From Goldberg and Suarez (2006).

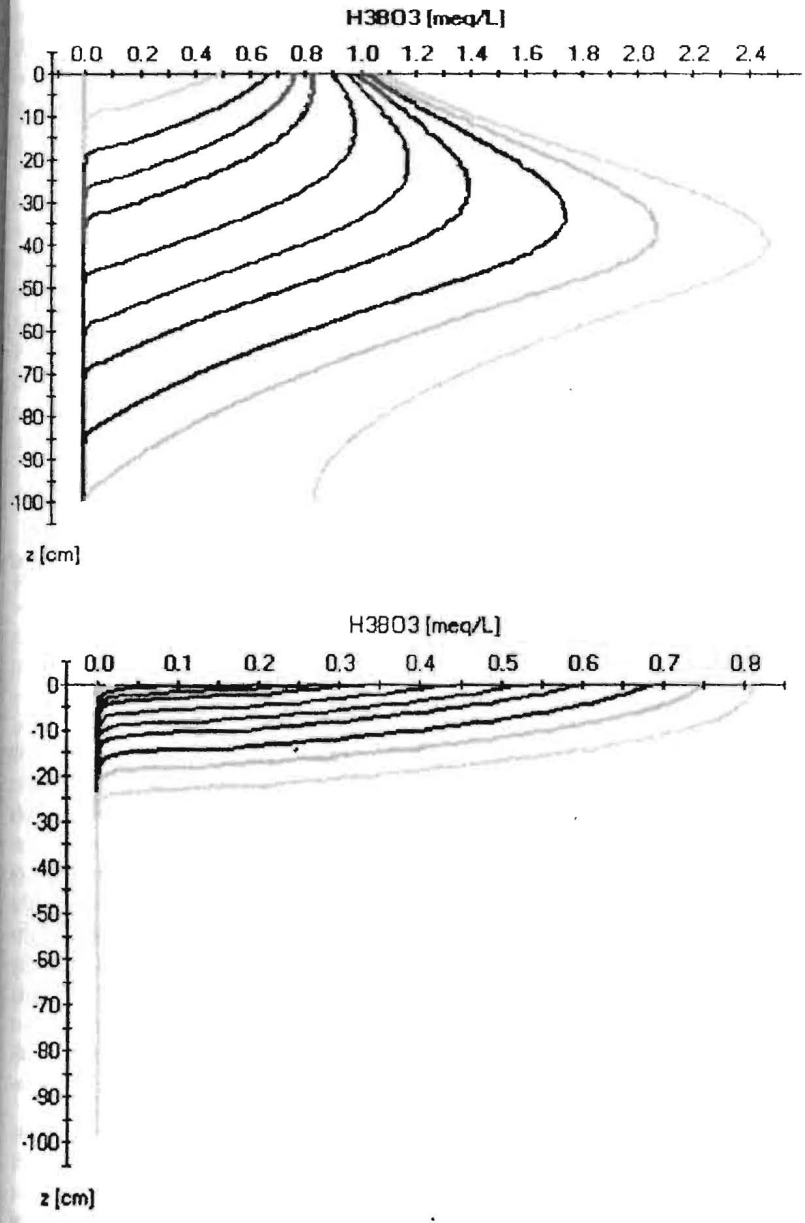

Figure 28-15. Change in boron concentration with depth and time (0, 10, 20, 30, 40, 50, 60, 70, 80, 90, and 100 days) for leaching fraction of 0.1 and soil surface area of (a) 100 m^2g^{-1}, and (b) 1,000 m^2g^{-1}. From Goldberg and Suarez (2006).

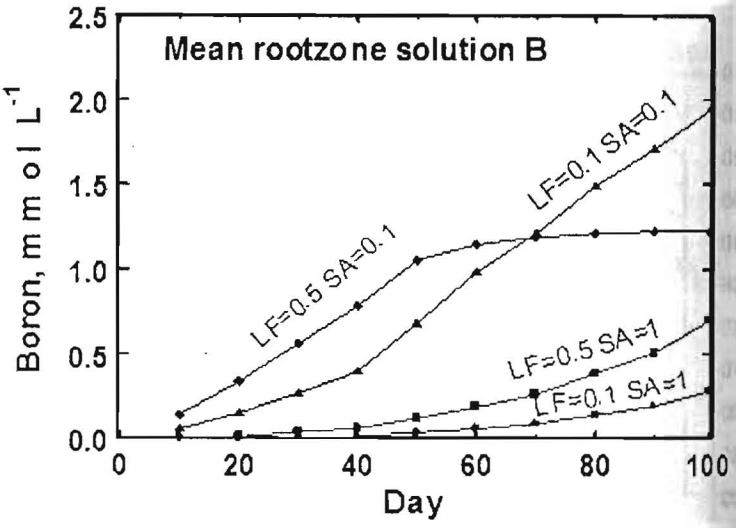

Figure 28-16. Mean root zone soil solution B concentration with time as related to leaching fraction (LF) and soil surface area (SA), expressed in $10^3 \times m^2 g^{-1}$. From Goldberg and Suarez (2006).

Plant Response to Salinity and Water Stress

As discussed, the *SWS* model predicts plant response to water and salt stress under dynamic conditions. The model uses the predicted decreases in plant water uptake to predict the decrease in biomass production. This calculation assumes that yield is directly proportional to water consumption (constant WUE, or water use efficiency). Improved predictions of yield loss can be obtained if the user has crop-specific information on the change in WUE as related to crop water consumption. Prediction of the yield of individual plant parts (such as seed or fruit) can be obtained by consideration of the relation of reduction in plant water uptake and yield response of the plant part of interest. The following example, taken in part from Suarez (2011), provides model predictions based on water stress, salt stress, and combined water and salt stress compared to steady-state predictions.

Scenario 1: No stress

In an initial simulation we examined crop production in the absence of matric or osmotic stress. A perennial crop with a 100-cm rootzone depth on a loam soil (k_s = 25 cm/day) was irrigated for 200 days. The first irrigation of 11 cm was applied after 10 days. After another 10 days, 22 cm of

water was applied over 2 days, followed by irrigations of 22 cm every 20 days thereafter, for a total of 209 cm of applied irrigation water. The potential ET of the crop for full yield was 200 cm and, for simplicity, we assumed a constant potential ET value of 1 cm/day. The crop was irrigated with a water of the following composition: Ca = 2 $mmol_c\ L^{-1}$, Mg = 1 $mmol_c\ L^{-1}$, Na = 10 $mmol_c\ L^{-1}$, Cl = 10.4 $mmol_c\ L^{-1}$, SO_4 = 1.4 $mmol_c\ L^{-1}$, and alkalinity = 0.2 $mmol_c\ L^{-1}$. The soil was initially at a moderate water content, with an input matric pressure of −100 cm at the surface and −85 cm at the 100-cm soil depth (the volumetric water content was calculated to be 0.244 at the surface and 0.257 at 100-cm depth). The $h_{\varphi 50}$ value for Eq. 28-14 was set at −150 m and p = 3. The model predicted 100% yield, with a water consumption of 200 cm, producing a calculated LF = 0.043. The steady-state calculation of salt stress would also predict no yield loss at this salinity level. When the salt stress value, $h_{\varphi 50}$ value was set to −50 m, we predicted a 99% relative yield.

Scenario 2: Matric stress

In this case we predict yield response to water stress. We irrigated a loamy sand soil (k_s = 356 cm/day) with the same root distribution, total water application, frequency daily ET, and water composition as in Scenario 1. Here we used an h_{50} value of −50 cm and p = 3 for the water stress response function (Eq. 28-13). The initial matric pressure was again −100 cm at the surface and −85 cm at the 100-cm depth (the volumetric water content was calculated to be 0.072 at the surface and 0.075 at the 100-cm depth). At the end of 200 days the model predicted a relative yield of 57%. The reduced yield is attributed to matric stress between irrigations on this loamy sand. The *SWS* model also predicted an LF value of 0.56, as compared to 0.043 with more frequent irrigation into the loam soil (Scenario 1). A steady-state model cannot predict the matric stress resulting from inadequate irrigation frequency and depending on soil properties, ET, and quantities of water applied. Thus, steady-state calculations cannot predict salt distribution, or the increased LF and drainage volume that results in these instances.

Scenario 3: Salt stress

We used the *SWS* model to predict plant yield reduction from salt stress. We utilized all the same conditions as in Scenario 1, with the exception of the water composition. We used the loam soil properties of Scenario 1. The initial soil water and irrigation water composition was as follows: Ca = 5 $mmol_c\ L^{-1}$, Mg = 5 $mmol_c\ L^{-1}$, Na = 50 $mmol_c\ L^{-1}$, Cl = 52 $mmol_c\ L^{-1}$, SO_4 = 7.0 $mmol_c\ L^{-1}$, and alkalinity = 1.0 $mmol_c\ L^{-1}$. The $h_{\varphi 50}$ for osmotic stress was set at −50 m. We set the h_{50} for matric stress to −50 cm to ensure that there was no matric stress. The predicted relative

yield was 62% and the predicted LF was 0.42. The increased leaching and decreased water uptake was due entirely to salt (osmotic stress).

The same scenario can be evaluated using the steady-state calculation as recommended by Ayers and Westcot (1985). In this calculation we consider the crop requirement of 200 cm of water and the applied water quantity of 209 cm. The EC of the irrigation water is estimated from the concentration and Eq. 3-11 (see Chapter 3 of this manual), yielding EC = 6.20 dS/m. The average rootzone salinity is calculated from the average salinity of the rootzone, using the irrigation water salinity and the salinity at the bottom of each of the four quarters of the rootzone.

The salinity is calculated for each quarter as $EC = EC_{iw}/LF_q$, where LF_q is the leaching fraction at the bottom of that quarter of the rootzone, using the assumption that water uptake is 40% in the first quarter, 30% in the second quarter, 20% in the third quarter, and 10% in the fourth quarter. In this case the salinity at the top is 6.2 dS/m and the salinity of the first through fourth quarters is 10.05, 18.8, 44.7, and 144.2 dS/m, respectively. The average rootzone salinity is calculated as 44.8 dS/m. Using Eq. 3-20 (see Chapter 3), this corresponds to calculated mean rootzone osmotic pressure of −179 m. Using the salt response of the crop utilized for these scenarios ($h_{\varphi 50} = -50$ m and $p = 3$), the mean osmotic pressure of −179 m, and applying Eq. 28-14, we calculate an $\alpha_\varphi(h_\varphi)$ value of 0.02. The predicted relative yield is thus 2% using the Ayers and Westcot (1985) calculation method.

A similar result would be obtained using the steady-state *WATSUIT* calculation. The major discrepancy between these calculations and the *SWS* predictions is the failure of these "traditional" calculations to predict the reduction in water consumption by the crop and, thus, the rootzone salinity and LF. Note that the LF was assumed to be 0.043 based on applied water and crop water demands (ET); however, the *SWS* model predicts reduced water uptake and an LF = 0.42. The differences between the model predictions (less stress) and the simple calculation method are even greater when we consider waters that precipitate gypsum in the soil, thus reducing the salt concentrations in the soil.

Scenario 4: Water and salt stress

In this scenario we again use the *SWS* model with the same conditions for water quantities, irrigation, potential ET, etc. The irrigation water composition was the same as used for Scenario 3 (salt stress only), with the difference being that this time we irrigated the loamy sand soil from Scenario 2 (matric stress only). If we were to simply combine the stresses by multiplying the independently calculated stress response functions, we would predict a relative yield of 35% (57% × 62%). The model prediction is 46% relative yield, accounting for the interaction of the stresses. In this case, the reduced water uptake by the salt stress reduced the soil

pressure head, thus reducing the matric stress. The reduced matric stress also allowed the salt concentrations and thus the salinity stress to be lower than would be expected by considering them separately.

The hazard with a static analysis and overly simplifying assumptions is also illustrated by the following calculations. A prediction of the outcome of Scenario 4 could be obtained by combining experimental observations under matric stress and the steady-state analysis of salt response. Adding the responses to both osmotic stress and matric stress together, without consideration of their interaction, would result in a predicted yield of only 19%.

Alternatively, if we were to add the water uptake averaged water matric and osmotic stress for Scenarios 2 and 3, we obtain an overall pressure of −138.5 m (−70.0 m from matric alone and −68.5 m from osmotic alone). Using Eq. 28-14 and combining the mean salt and matric pressure with an h_{50} of −50 m would give a predicted relative yield of only 4.5%. As discussed in Scenario 2, the static calculation without correction for reduced water uptake would predict a 2% yield based on salt stress alone.

Although the preceding example is somewhat extreme in terms of the close correspondence between water application and crop water demand (209 cm vs. 200 cm), such irrigation efficiency is not unusual for new irrigation technologies, such as drip irrigation. It appears that dynamic modeling is necessary for irrigation management when low target LFs are the objective under conditions of potential yield loss due to salinity.

SUMMARY

The *SWS* model is a variation on the *UNSATCHEM* model (Suarez and Šimůnek 1992, 1997) with addition of calculations for ET, a new B adsorption routine, and with a user-friendly interface that makes extensive use of default parameters to minimize the need for user expertise in soil physics and chemistry. The *SWS* model accounts for a number of functions and processes known to influence practical aspects of irrigation and drainage management, including:

- Hydraulic functions
- Chemical effects on HC
- Water uptake by plant roots, including an optional root growth function
- Calculations of crop ET
- Factors controlling soil CO_2 concentrations (production and transport)
- Soil-water chemistry (transport, osmotic pressure, chemical activity, calcite precipitation, gypsum content, magnesium precipitation, cation exchange, boron).

Based on comparisons of the model simulations and reliable, readily available field data, the *SWS* model predicts actual field conditions with reasonable accuracy:

- Soil water content and soil CO_2
- EC and SAR
- Reclamation effects of various alternatives amendments (such as gypsum, organic matter, and/or acid dissolution of calcite, alone or in combination), including secondary effects such as increases in pH or salt loading
- Effects of rain on soil SAR
- Effects management protocols for boron in soils with variable leaching fractions
- Plant response to various salinity and water stress combinations.

The comparison of field results to results of *SWS* simulations suggests that transient models like the *SWS* model may provide more accurate and precise predictions of actual field soil and water conditions as a result of irrigation and other soil management inputs than are feasible with more traditional steady-state prediction models. This greater predictive ability of such models is obtained with input data that are often readily available from routine on-farm measurements. This type of dynamic modeling may be necessary for irrigation management when low target LFs are the objective under conditions of potential yield loss due to salinity.

REFERENCES

Addiscott, T. M., and Wagenet, R. J. (1985). "Concepts of solute leaching in soils: A review of modeling approaches." *J. Soil Sci.*, 85, 411–424.

Allen, R. G., Peieira, L. S., Raes, D., and Smith, M. (1998). *Crop evapotranspiration*, FAO Irrigation and Drainage Paper 56, Food and Agriculture Organisation of the United Nations, Rome.

Ayers, R. S., and Westcot, D. W. (1985). *Water quality for agriculture*, FAO Irrigation and Drainage Paper 29, Rev. 1 Food and Agriculture Organisation of the United Nations, Rome.

Bresler, E. (1973). "Simultaneous transport of solutes and water under transient unsaturated flow conditions." *Water Resour. Res.*, 9, 975–986.

Buyanovsky, G. A., and Wagner, G. H. (1983). "Annual cycles of carbon dioxide level in soil air." *Soil Sci. Soc. Am. J.*, 47, 1139–1143.

Carsel, R. F., and Parrish, R. S. (1988). "Developing joint probability distributions of soil water retention characteristics." *Water Resour. Res.*, 24, 755–769.

Dutt, G. R. (1962). "Prediction of the concentration of solutes in soil solutions for systems containing gypsum and exchangeable Ca and Mg." *Soil Sci. Soc. Am. Proc.*, 26, 341–343.

Dutt, G. R., Shaffer, M. J., and Moore, W. J. (1972). *Computer simulation model for dynamic bio-physical processes in soils*, University of Arizona Agricultural Experiment Station Bulletin, Tucson, Ariz.

Felmy, A. R. (1990). *GMIN: A computerized chemical equilibrium model using a constrained minimization of the Gibbs free energy*, Pacific Northwest Lab, Richland, Wash.

Goldberg, S. R., and Glaubig, R. A. (1986). "Boron adsorption on California soils." *Soil Sci. Soc. Am. J.*, 50, 1173–1176.

Goldberg, S. R., Lesch, S. M., and Suarez, D. L. (2000). "Predicting boron adsorption by soils using the soil chemical parameters in the constant capacitance model." *Soil Sci. Soc. Am. J.*, 64, 1356–1363.

Goldberg, S., and Suarez, D. L. (2006). "Prediction of anion adsorption and transport in soil systems using the constant capacitance model," in *Surface complexation modeling*, J. Luetzenkirchen, ed., Interface Science and Technology Series, Elsevier, Amsterdam, 11, 491–517.

Grieve, C. M., Maas, G., and Grattan, S. (2011). "Plant salt tolerance," in *Agricultural salinity assessment and management*, Chapter 13, this volume.

Hanks, R. J., and Bowers, S. A. (1962). "Numerical solution of the moisture flow equation for infiltration into layered soils." *Soil Sci. Soc. Am. Proc.*, 26, 530–535.

Herbelin, A. L., and Westall, J. C. (1996). *FITEQL: A computer program for determination of the chemical equilibrium constants from experimental data*, Report 96-01, Ver. 3.2, Dept. of Chemistry, Oregon State University, Corvallis, Ore.

Inskeep, W. P., and Bloom, P. R. (1986). "Kinetics of calcite precipitation in the presence of water soluble organic ligands." *Soil Sci. Soc. Am. J.*, 50, 1167–1172.

Labadie, J. W., and Khan, I. A. (1979). "River basin salinity management via the ASTRAN method, I: Model development." *J. Hydrol.*, 42, 301–321.

Lebron, I., and Suarez, D. L. (1996). "Calcite nucleation and precipitation kinetics as affected by dissolved organic matter at 25 °C and pH >7.5." *Geochem. Cosmochim Acta*, 60, 2767–2776.

Logan, S. H., and Boyland, P. B. (1983). "Calculating heat units via a sine function." *J. Am. Soc. Hort. Sci.*, 108, 977–980.

Maas, E. V., and Hoffman, G. J. (1977). "Crop salt tolerance: Current assessment." *J. Irrig. Drainage Div. ASCE*, 103(IR2), 115–134.

McNeal, B. L. (1968). "Prediction of the effect of mixed-salt solutions on soil hydraulic conductivity." *Soil Sci. Soc. Am. Proc.*, 32, 190–193.

Pitzer, K. S. (1973). "Thermodynamics of electrolytes I: Theoretical basis and general equations." *J. Phys. Chem.*, 77, 268–277.

——. (1979). *Activity coefficients in electrolyte solutions*, Chapter 7, CRC Press, Boca Raton, Fla.

Quilez, D., Isidoro, D., and Aragüés, R. (2011). "Conceptual irrigation project hydrosalinity model," in *Agricultural salinity assessment and management*, Chapter 30, this volume.

Robbins, C. W., Wagenet R. J., and Jurinak J. J. (1980). "A combined salt transport-chemical equilibrium model for calcareous and gypsiferous soils." *Soil Sci. Soc. Am. J.*, 44, 1191–1194.

Shainberg, I., and Levy, G. J. (1992). "Physico-chemical effects of salts upon infiltration and water movement in soils," in R. J. Wagenet, P. Baveye, and B. A. Stewart, eds., *Interacting processes in soil science*, Lewis Publishers, CRC Press, Boca Raton, Fla.

Šimůnek, J., and Suarez, D. L. (1993). "Modeling of carbon dioxide transport and production in soil: 1. Model development." *Water Resour. Res.*, 29, 487–497.

Stokes, R. H. (1979). "Thermodynamics of solutions," in *Activity coefficients in electrolyte solutions*, R. M. Pitkowicz, ed., CRC Press, Inc., Boca Raton, Fla.

Suarez, D. L. (1977). "Ion activity products of calcium carbonate in waters below the rootzone." *Soil Sci. Soc. Am. J.*, 41, 310–315.

———. (2001). "Sodic soil reclamation: Model and field study." *Aust. J. Soil Res.*, 39, 1225–1246.

———. (2011). "Soil salinization and management options for sustainable crop production," in *Handbook of crop and plant stress*, 3rd ed., M. Pessarakli, ed., CRC Press, Boca Raton, Fla.

Suarez, D. L., and Dudley, L. (1998). "Hydro chemical considerations in modeling water quality within the vadose zone," in *Agroecosystems and the environment: Sources, control, and remediation of potentially toxic trace element oxyanions*, L. Dudley and J. Guitjens, eds., American Association for the Advancement of Science–Pacific Division, San Francisco University, San Francisco, Calif.

Suarez, D. L., Rhoades, J. R., Lavado, R., and Grieve, C. M. (1984). "Effect of pH on saturated hydraulic conductivity and soil dispersion." *Soil Sci. Soc. Am. J.*, 48, 50–55.

Suarez, D. L., and Šimůnek, J. (1992). *The* UNSATCHEM *code for simulating one-dimensional variably saturated water flow, heat transport, carbon dioxide production and transport, and multicomponent solute transport with major ion equilibrium and kinetic chemistry, Ver 1.1*, Research Report No. 129, U.S. Salinity Laboratory, USDA-ARS, Riverside, Calif.

———. (1993). "Modeling of carbon dioxide transport and production in soil: 2. Parameter selection, sensitivity analysis and comparison of model predictions to field data." *Water Resour. Res.*, 29, 499–513.

———. (1996). "Solute transport modeling under variably saturated water flow conditions," in *Reactive transport in porous media, reviews in mineralogy*, Vol. 34, P.C. Lichtner, C.I. Steefel, and E. H. Oelkers, eds., Mineralogical Society of America, Washington, DC.

———. (1997). "*UNSATCHEM:* Unsaturated water and solute transport model with equilibrium and kinetic chemistry." *Soil Sci. Soc. Am. J.*, 61, 1633–1646.

Suarez, D. L., and Wood, J. W. (1993). "Predicting Ca-Mg exchange selectivity of smetitic soils," in *Agronomy Abstracts*, American Society Agronomy, Madison, Wisc., 236.

Suarez, D. L., Wood, J. W., and Ibrabim, I. (1992). "Reevaluation of calcite supersaturation in soils." *Soil Sci. Soc. Am. J.*, 56, 1776–1784.

Suarez, D. L., Wood, J. W., and Lesch, S. M. (2006). "Effect of SAR on water infiltration under a sequential rain-irrigation management system." *Agric. Water Mgmt.*, 86, 150–164.

Truesdell, A. H., and Jones, B. F. (1974). "*WATEQ*, a computer program for calculating chemical equilibria of natural waters." *J. Res. U.S. Geol. Surv.*, 2, 233–248.

van Genuchten, M. T. (1980). "A closed-form equation for predicting the hydraulic conductivity of unsaturated soils." *Soil Sci. Soc. Am. J.*, 44, 892–898.

——. (1987). *A numerical model for water and solute movement in and below the root-zone*, unpublished research report, U.S. Salinity Laboratory, USDA-ARS, Riverside, Calif.

Wagenet, R. J., and Hutson, J. L. (1987). LEACHM: *Leaching estimation and chemistry model, Continuum* 2, Water Resources Institute, Cornell University, Ithaca, New York.

White, N., and Zelazny, L. W. (1986). "Charge properties in soil colloids," in *Soil physical chemistry*, D. L. Sparks, ed., CRC Press, Boca Raton, Fla., 39–81.

ASCE Manuals and Reports on Engineering Practice No. 71

Agricultural Salinity Assessment and Management, Second Edition

Prepared by the Water Quality Technical Committee of
the Irrigation and Drainage Council of
the Environmental and Water Resources Institute
of the American Society of Civil Engineers

Edited by
Wesley W. Wallender, Ph.D., P.E., and Kenneth K. Tanji, Sc.D.

ASCE AMERICAN SOCIETY OF CIVIL ENGINEERS

EWRI ENVIRONMENTAL & WATER RESOURCES INSTITUTE